Influence of permafrost type and site history on losses of permafrost carbon after thaw

Kristen L. Manies[1*], Miriam C. Jones[2], Mark P. Waldrop[1], Mary-Cathrine Leewis[1], Christopher Fuller [1], R. Scott Cornman[3], and Kristen Hoefke[2]

[*]Corresponding author

[1]U.S. Geological Survey; Geology, Minerals, Energy, and Geophysics Science Center; Menlo Park, CA

[2]U.S. Geological Survey; Florence Bascom Geoscience Center; Reston, VA

[3]U.S. Geological Survey; Fort Collins Science Center; Fort Collins, CO

Key points

- Collapse-scar bog ages at our sites were not related to feature size and may have been more influenced by local factors.
- We found smaller losses of C with permafrost thaw than other studies from Interior Alaska.
- The timing of permafrost aggradation relative to peat accumulation is an important factor in determining how much C is lost with thaw.

Abstract

We quantified permafrost plateau and post-thaw carbon (C) stocks across a peatland permafrost thaw chronosequence in Interior Alaska to evaluate the amount of C loss with thaw. Peat core macrofossil reconstructions revealed three stratigraphic layers of peat: (1) a base layer of fen/marsh peat, (2) forested permafrost plateau peat and, (3) collapse-scar bog peat (at sites where permafrost thaw has occurred). Radiocarbon dating revealed that peat initiated at all sites within the last 2,500 years and that permafrost aggraded during the Little Ice Age (ca. 250 – 575 years ago) and degraded within the last several decades. We found the timing of permafrost thaw within each feature was not related to thaw bog size, as hypothesized. Their rate of expansion may be more influenced by local

factors, such as ground ice content and subsurface water inputs. We found C losses due to thaw for the century of approximately 34% of the C available, but the absolute amount of C lost (kg m^{-2}) was over 50% lower than losses previously described in other Alaskan peatland chronosequences. We hypothesize that the difference stems from the process by which permafrost aggraded, with sites that formed permafrost epigenetically (significantly later than the majority of peat accumulation) experiencing less C loss with thaw than sites that formed syngenetically (simultaneously with peat accumulation). We suggest that C:N ratios can provide a first order estimate of how much peat has been processed prior to permafrost aggradation, helping to predict the magnitude of C loss with thaw.

Plain Language Summary

We quantified peat carbon at a permafrost peatland in Alaska to see how much carbon was lost from the peat when permafrost, or frozen soil, thawed and that area became a collapse-scar bog. We found that size of the bog was unrelated to its age. Factors such as the amount of ice in the soil and water entering the bogs from the surrounding forests may have been more important in determining their growth. We did not find as large of losses of carbon from as found at other Alaskan sites. We compared our results to other studies, some which had small losses of carbon due to thaw, others which found large losses. We found that factors related to time (i.e., age of landform, number of years the site had permafrost) are important but don't fully explain these different results. However, when we include how permafrost formed we see a trend: sites where permafrost formed after peat (epigenetic permafrost) had smaller carbon losses than sites where permafrost and peats formed at the same time (syngenetic permafrost). Determining permafrost type can be difficult; instead scientists can use C:N ratios to determine if their samples resemble peat formed by epigenetic versus syngenetic permafrost.

1.0 Introduction

Northern peatlands play an important role in the global carbon (C) budget and are estimated to store 415 Pg of C (+/- 150 Pg C; Hugelius et al., 2020), which represents approximately 20 % of the global soil C stock (Jackson et al., 2017). Close to half of this C has been protected from decomposition by permafrost, substrate that has remained frozen for at least two consecutive years (Rodenhizer et al., 2020). Permafrost in northern peatlands reached its maximum extent around 1700 Common Era (CE), with the highest rates of aggradation between 1200 - 1950 CE (Treat & Jones, 2018). Much of this permafrost is found in the discontinuous zone, where areas of permafrost are found adjacent to areas of unfrozen soil. In the discontinuous zone, the majority of which resides above 60 °N (Brown et al., 1997), the presence of permafrost depends on the area's climate (both past and present) as well as local factors, such as vegetation, aspect, thickness of organic soil horizons, and texture of the mineral soil (Shur & Jorgenson, 2007). Permafrost can form either after the deposition of peat/sediments (epigenetic permafrost) or concurrent with peat/sediment deposition (syngenetic permafrost). Between 2.20 – 3.95 10^6 km^2 of the northern hemisphere is estimated to have discontinuous permafrost (Zhang et al., 2000).

Permafrost peatlands within the discontinuous zone are often associated with forested peat plateaus (Gibson et al., 2019). Typically, these ecosystems are vegetated with black spruce (*Picea mariana*) trees and ericaceous shrubs, such as Labrador Tea (*Rhododendron groenlandicum*), with a ground cover of feathermosses and *Sphagnum* spp. The underlying organic soil, or peat, can be up to 6 m thick (Gibson et al., 2019). The uppermost peat, known as the active layer, undergoes seasonal freezing and thawing and is usually 0.3 – 0.7 m thick, with permafrost found below (Shur et al., 2011). Microbial decomposition of organic matter (OM) in this frozen soil is dramatically reduced compared to unfrozen soils, thereby stabilizing a large pool of potentially labile C (Harden et al., 2012; Leewis et al.,

2020). Once thawed, this reserve of C is available for more rapid decomposition, which results in losses of C from the soil, much of which is lost to the atmosphere.

Over the past few decades, air temperatures within the northern high latitudes have warmed at a faster rate than other locations around the globe (Oliva & Fritz, 2018). These changes have increased soil temperatures (Jungqvist et al., 2014), growing-season length (Euskirchen et al., 2009), and both fire frequency and intensity (Turetsky et al., 2011), all of which impact permafrost stability and C storage within these landscapes. In well drained sites, post-thaw conditions usually result in water draining from the soil, resulting in oxic soil conditions (Estop-Aragonés et al., 2018a). However, permafrost thaw in lowlands often results in subsidence and inundation, changing the ecosystem from a relatively dry forested permafrost plateau to bogs or fens with a near-surface water table (Schuur et al., 2015), resulting in a soil profile that is primarily anaerobic or microaerobic.

In lowlands, transitioning from a forested peat plateau to an inundated wetland impacts C cycling in several ways. First, this transition results in wholesale changes in vegetation; trees die as their roots become inundated with ground subsidence, resulting in a shift in dominance to inundation-tolerant *Sphagnum* and/or *Carex* spp. (Finger et al., 2016). Increases in the amount of *Sphagnum* impacts C accumulation rates (Thormann et al., 1999), as *Sphagnum* is known to reduce decomposition through lowered pH and creation of decay resistant litter (Malmer et al., 2003). In addition, although thawed OM is more available to microbial decomposition, inundation creates an anaerobic low nutrient environment, which shifts microbial populations towards less efficient anaerobic metabolism and the production of CH_4 rather than CO_2 (Treat et al., 2014). When present, *Carex* spp. are known to increase diffusion of these gases to the atmosphere from deeper in the soil profile through their aerenchymatous tissues (Waldo et al., 2019).

Permafrost thaw and the formation of collapse scar bogs alters net ecosystem exchange (NEE), as evidence by the amount of C stored within peat. Some studies have found large C losses from thawed

permafrost peat (Jones et al., 2017; O'Donnell et al., 2012) and suggest that it may take centuries to millennia for these C stocks to recover to their pre-thaw stocks. However, other studies have shown little C loss from previously frozen peat (Estop-Aragonés et al., 2018a; Heffernan et al., 2020), such that these losses could be relatively quickly offset by post-thaw peat accumulation. To further understand the factors which might determine the magnitude of C lost upon permafrost thaw, this study examines C losses for a new thaw chronosequence situation within forested permafrost plateaus at a site located in Interior Alaska. We calculate the amount of C loss with thaw for this site and examine these results in context of other similar studies to understand the factors driving C loss rates.

2.0 Methods

2.1 Site information

This study took place in the Alaska Peatland Experiment (APEX; Figure 1), located within the lowlands of the Bonanza Creek Long-term Ecological Research (LTER) site, on the northwest side of the Tanana River, a glacially fed braided river. The average annual temperature for this part of Interior Alaska is -2.4 ^{o}C (1981 – 2010), with the average January and July temperatures being -22.2 ^{o}C and 16.9 ^{o}C, respectively (https://www.ncdc.noaa.gov/cdo-web/datatools/normals; Fairbanks, AK). This region receives ~285 mm of precipitation per year, with about one-third occurring during the winter months (Hinzman et al., 2006). This region is also within the area of discontinuous permafrost; therefore, permafrost tends to be found on north facing slopes, valley bottoms, and lowlands (Brown & Kreig, 1983).

The study area is dominated by forested permafrost peat plateaus, covered with *Picea mariana,* ericaceous shrubs, feather mosses, and occasional *Eriophorum* spp. in the wetter areas. These plateaus are broken up by collapse-scar bogs of varying sizes (5 – 15,000 m^2). Collapse-scar bogs form when localized permafrost thaws; these wetlands remain surrounded by permafrost plateaus, with deeper permafrost below, isolating the thawed bog from groundwater. Vegetation of these bogs is

characterized by diverse *Sphagnum* and *Carex* spp. plants. We examined three thaw features within the study area, assumed to have thawed at different times in the past based on their size and surface vegetation. One thaw feature (~1,300 m^2), with no visible dead trees, was assumed to have thawed longer ago (Figure 1, red outline, BZSE) than a second feature (~2,000 m^2) that had drunken or dead trees on the surface (Figure 1, blue outline, BZBT). A much smaller feature (~50 m^2) was assumed to have initiated thaw within the past few decades (Figure 1, yellow outline, BZBB). These sites were assumed to represent a chronosequence of thaw, ranging from "old" (thaw thought to occur over centuries), "intermediate" (thaw over decades), and "young" (thaw within the past decade) bogs, following previous chronosequence studies (Jones et al., 2017; O'Donnell et al., 2012).

2.2 Soil core collection and analysis

Two to four cores were collected at each site, with method depending upon ecosystem type and time of sampling. Frozen soil was cored with a Snow, Ice, and Permafrost Research Establishment (SIPRE) corer (~7.6 cm diameter; Rand & Mellor, 1985). Unfrozen material was usually collected using a 'frozen finger'. Here, a thin-walled, hollow aluminum tube (~6.5 cm diameter), sealed at one end, was inserted into the peat to the mineral soil. A slurry of dry ice and ethanol was poured into the corer, freezing the surrounding material to the outside of the corer. After removal the exterior of the core was scraped to remove large roots and any foreign material that became frozen to the core during removal. Both SIPRE cores and frozen finger cores were taken to at least the peat-mineral soil boundary. Because the frozen finger corer did not always recover the surface ~20 cm of peat very well, we sometimes sampled surface material by removing the surface peat in blocks of known dimensions (peat monolith). When more than one method was used to collect a core, sample data were later combined to represent an entire soil profile. In all cases, cores were subsampled into 2 to 5 cm depth increments.

Processing steps for each subsample depended on the type of sample. Most SIPRE subsamples, which were a circular disk-shape, were divided into four quadrants used for: 1) chemistry (C, nitrogen

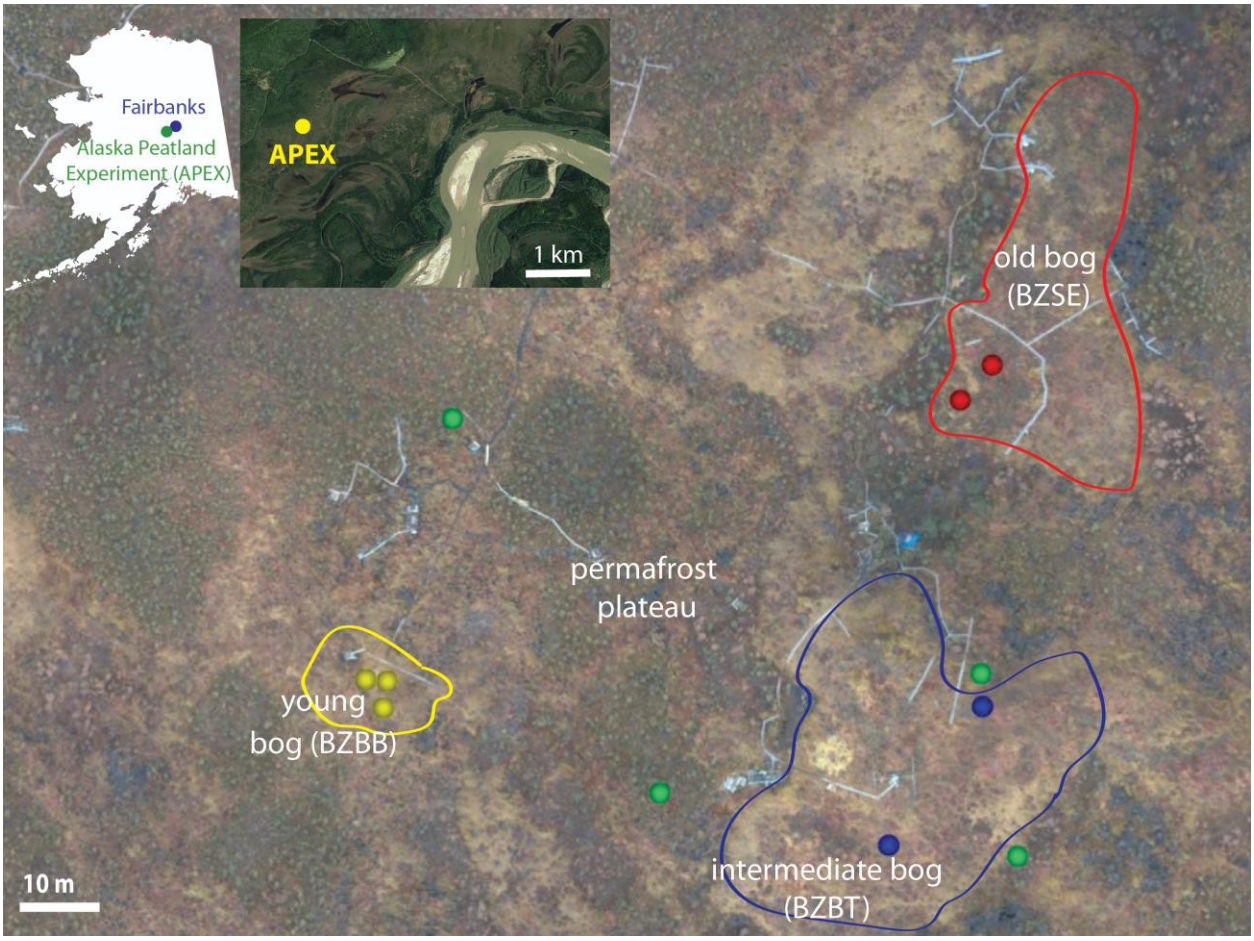

Figure 1. *The Alaskan Peatland Experiment (APEX) site. This area is a mosaic of collapse-scar bogs within forested permafrost plateaus. Colors correspond to the different bogs: the 'old' bog is in red (BZSE), the 'intermediate' bog is in blue (BZBT), and the 'young' bog is in yellow (BZBB). Circles indicate the locations of the soil cores; green circles are cores taken from the permafrost plateau. Core numbers can be found in Figure S2. APEX is located near Fairbanks, close to the Tanana River, in the Interior of Alaska. Images: site - J. Hollingsworth; satellite – Google Earth.*

(N), and ^{210}Pb) and bulk density, 2) macrofossil and ^{14}C analysis, 3) DNA-based plant community assessment, and 4) an archive. Volume of the bulk density quadrant was determined by first calculating the area the quadrant (0.25 * area of a circle) averaging several measurements of the radius (using digital calipers) and multiplying this value by the average of several measurements of the disk thickness. Bulk density samples were then weighed, oven dried (65 °C for organic samples, estimated to have > 20% OM; 105 °C for mineral soils), weighed again, and ground to pass through a 0.25 mm screen for further analyses (see following paragraph). For other SIPRE subsamples the disk was trimmed into

155 the shape of a rectangle, the dimensions of which were measured using digital calipers, with the
156 remainder of the core saved for other analyses and an archive. Frozen finger samples had at least three
157 small rectangular cubes cut from the larger sample, the dimensions of which were measured using
158 digital calipers. The remainder of the frozen finger subsample was split between macrofossil analyses
159 and an archive. The rectangular prisms from both the SIPRE and the frozen finger methods were dried
160 and ground in the same manner as described above. Regardless of sample collection method, all
161 samples were described using visual and tactical factors such as level of decomposition, color, and root
162 abundance. Based on these descriptions they were assigned a horizon designation: live moss (L), dead
163 moss (D), fibric (mostly undecomposed plant material, F), mesic (more decomposed plant material, M),
164 humic (very decomposed plant material, H), and mineral soil (Min) based on Manies et al. (2020).
165 The chemistry sample was analyzed for total C and N using a Carlo Erba NA1500 elemental
166 analyzer (ThermoScientific, Waltham, MA). Samples were combusted in the presence of excess oxygen.
167 The resulting sample gases were carried by a continuous flow of helium through an oxidation furnace,
168 followed by a reduction furnace, to yield CO_2, N_2, and water vapor. Water was removed by a chemical
169 trap and CO_2 and N_2 were chromatographically separated before the quantification of C and N (Pella,
170 1990a, 1990b). Because carbonates are generally absent in this area and pH values were generally less
171 than 6.0, it was assumed that there was no inorganic carbon present in the mineral soil samples (Soil
172 Survey Staff, 1951), and, thus, total C represents total organic C. More detailed information regarding
173 sample processing for samples from the intermediate bog can also be found in Manies et. al (2017). C
174 storage for each subsample was calculated using C concentration (%), bulk density (g cm^{-3}), and
175 thickness (cm) data. C stocks (kg m^{-2}) were calculated as cumulative C storage for all samples between
176 the moss surface and the organic-mineral soil interface. Examinations of C stocks versus the number of
177 years for which the core had that stratum (i.e., was a fen, had permafrost) were performed using the *nls*
178 and *lm* commands in R (R Core Team, 2017).

To date surface soil layers, we measured both ^{14}C in plant macrofossils (see below) and ^{210}Pb in bulk soil. ^{210}Pb, bound to aerosols and dust particles, has been deposited on the land surface from atmospheric fallout, largely during precipitation events. Age dating using this radionuclide assumes that ^{210}Pb does not migrate downward within the soil profile over time, so that the activity found at depth reflects its decay since time of deposition. To examine if ^{210}Pb was migrating we collected additional surface soil samples for which we measured both ^{210}Pb and ^{7}Be. Because ^{7}Be is also deposited atmospherically but has a much shorter half-life (53 days versus 22 years), we used ^{7}Be as a tracer to estimate the amount of downward transport, or "downwash", of ^{210}Pb. Radionuclides ^{210}Pb, ^{226}Ra, ^{137}Cs, and ^{7}Be were measured on dried, ground samples (2 to 5 cm thick intervals) using gamma spectrometry following methods described in Van Metre and Fuller (2009). Samples from each soil profile were measured until unsupported ^{210}Pb, defined as the activity greater than the activity of its long-lived parent ^{226}Ra, was not detected. Unsupported ^{210}Pb is largely from atmospheric deposition. The Constant Rate of Supply (CRS) method was used to calculate ages and associated uncertainties from unsupported ^{210}Pb and were calculated as a function of cumulative dry mass (g cm^{-2}) instead of depth to account for compaction (Van Metre & Fuller, 2009). Although ^{137}Cs was measured (data available in Manies et al., 2021), it was not used to date soil layers due its mobility in acidic peat and potential biological uptake by vegetation (Turetsky et al., 2004).

2.3 Macrofossil analysis

Plant macrofossil assemblages were used as evidence for transitions from one state to another, such as a forested permafrost plateau to a collapse-scar bog. Approximately 2 cc of sample was washed through a 250 µm screen using deionized water and examined under a microscope to identify dominant peat types using semi-quantitative methods (Yu et al., 2010). Relative abundances of herbaceous, ligneous, and bryophytic peat were estimated and seeds, needles, leaves, and other distinct plant macrofossils were tallied. Based on characteristics of macrofossil assemblages (Treat et al., 2016), we

classified the peat into several categories: 1) 'herbaceous'-dominated peat, containing remains of Cyperaceae (sedges); 2) 'ligneous' (woody) peat assemblages, which included evidence for taxa such as black spruce (*Picea mariana*), shrubs, and bryophyte taxa (e.g., feathermosses) associated with hummocks; and 3) 'bryophytic' peat, which was dominated by *Sphagnum* and other brown mosses. Where possible, *Sphagnum* mosses were identified to section level and brown mosses were identified to genus or species level. Brown mosses were further categorized based on their habitat. For example, mosses in the Amblystegiaceae family are associated with inundated environments, while feather mosses, *Tomenthypnum nitens,* and *Aulacomnium palustre* were grouped into a 'dry' (hummock or permafrost plateau) category. Unidentifiable detritus, or plant remains that were too decomposed to identify their provenance, was also included when present. Zones of permafrost aggradation (a transition from fen/marsh peat to permafrost plateau peat, see Results) were identified using a decrease in herbaceous peat with a corresponding increase in ligneous peat. Zones of permafrost thaw (collapse scar bog peat) were identified using an increase in bryophytic peat with a corresponding decrease in ligneous peat. Transitions between peat types were identified using visual inspections of the macrofossil data and confirmed with CONISS based cluster analysis using the Tilia program, which clusters samples based on presence and abundance of taxa in each sample (v 2.6.1; Grimm, 1987). Core sections with "dry" mosses, even in small percentages, were assigned to the permafrost plateau strata. Note that macrofossil horizon designations are not synonymous with field-based horizon designations (e.g. fibric, mesic, humic).

Macrofossil material was used to obtain radiocarbon (^{14}C) ages of initial peat formation (landform initiation), permafrost aggradation, and permafrost degradation rates in each core. We picked terrestrial plant macrofossils (seeds, leaves, needles and charcoal) from the sieved macrofossil samples, targeting the depths of transition in macrofossil assemblage. The ^{14}C content of each sample was measured by accelerator mass spectrometry at either the Lawrence Livermore National Laboratory

Center for Accelerator Mass Spectrometry (CAMS) or at Beta Analytic (Miami, FL; see Table S2 for details). Additional information regarding ^{14}C processing can be found in Manies et. al (2017). Radiocarbon ages were calibrated to calendar ages in calendar years before present (cal yr BP; present = 1950 CE) and age models were generated using Bacon v 2.3.9.1 (Blaauw & Christen, 2011).

2.4 C loss over time

Cores can have variable amounts of C in their permafrost strata for two reasons: 1) loss due to thaw, and 2) differing amounts of time for which a core had permafrost, which affects the total amount of forest permafrost plateau C that a core was able to accumulate. We accounted for the variable times for which cores had permafrost in two ways. The first method normalizes the C stocks of thawed cores based on the amount of time each core was accumulating both fen/marsh and forested permafrost plateau peat to the longest amount of time a core was recorded as accumulating these peats (2725 yrs). For example, the time for which the Young-bog 2 core (BB2) was accumulating both fen/marsh and forested permafrost plateau peat was 2040 yrs, or 75 % of 2725 yrs. Therefore, we increased the C stocks of the BB2 core by 25%, thus accounting for any differences in stocks that may have occurred due to differences in time with permafrost, with the assumption that any remaining differences in C stocks are due to thaw-based C losses. We are calling this process the “Normalized C” method. Confidence intervals were determined using the R package *plotFit* (Greenwell & Schubert Kabban, 2014).

The second method we used to account for C stock differences was also used by Jones et al. (2017). In this method two linear relationships between C stocks versus time (years with fen and permafrost peat) are calculated for 1) for the cores for which permafrost is still present, and 2) for the cores for which permafrost has thawed. The difference between these two slopes indicates the degree to which C has been lost with thaw. We are calling this process the “slope comparison” method.

2.5 Plant DNA Extraction, Amplification, and Analyses

We used DNA based techniques to assess the relative abundance of plant DNA (Alsos et al., 2016; Taberlet et al., 2006), and compared it to morphologically-based macrofossil count data for four cores. We tested the usefulness of the DNA based technique as a high throughput option of determining vegetation transitions from these peat cores, which occurred relatively recently. For each of the four cores for which both macrofossils and DNA analysis was performed, we extracted total genomic environmental DNA (eDNA) from 44 samples, between 7-10 subsamples for each core from both above and below the macrofossil-identified transition from forested peat plateau to bog, along with eight negative controls (one negative control for each 5 core samples processed). To mitigate the potential for sample contamination by modern plant DNA, the outer 0.5 cm of each core was scraped off using sterile tools prior to DNA extraction (sensu Leewis et al., 2020). Prior to core cleaning, all nearby surfaces were sterilized using 10% bleach followed by 70% ethanol spray. Cores and subsets for DNA extraction were handled only on sterile aluminum foil and all tools (i.e. scalpels, tweezers, foil) were sterilized prior to use and between each core; additionally, updraft created by an open Bunsen flame was used to limit infall of potentially contaminating DNA. Negative controls consisted of sterile molecular grade water in an open tube near the DNA extraction station and were carried throughout the entire analysis including DNA extraction, PCR, and sequencing. Whole genome eDNA was extracted from ~0.5 g of permafrost using the DNeasy PowerSoil Kit (Qiagen, Redwood City, CA) according to the manufacturer's instructions. All samples were eluted into 30 µL of molecular grade water. DNA quantity was assessed using a PicoGreen dsDNA Assay Kit (Thermo Fisher Scientific Technologies, Wilmington, DE) and concentrations ranged from 9 to 25 ng uL^{-1}. All PCR amplifications were performed with the *g* (5'-GGGCAATCCTGAGCCAA-3') and *h* (5'-CCATTGAGTCTCTGCACCTATC-3') universal plant primers for the short and variable P6 loop region of the chloroplast *trnL* intron (Taberlet et al., 2006), with addition of index adapters as required by the RTSF Genomics Core (https://rtsf.natsci.msu.edu/genomics/tech-

notes/amplicon-metagenomic-guide/). The amplification was conducted using the following conditions: 97 °C for 4 min, followed by 35 cycles of 94 °C (45 s), 56.7 °C (45 s), and 72°C (45 s), with a final extension at 72°C (10 min). The amplification was performed in a 25 µL mixture containing 0.25 µL Taq (5U, AmpliTaq Gold, Thermo Fisher Scientific), 5 µL 5X buffer, 1.5 µL MgCl2 (25 mM), 0.5 µL dNTPs (10 mM), 0.25 µL BSA (10 mg mL^{-1}), 0.25 µl of each primer (50 µM), 5 µl of DNA template (ca. 5 ng uL^{-1}), and 12 µL of nuclease- free water. Amplicons were visualized in a 2 % agarose gel. Amplicons were then purified using the DNA Clean and Concentrator-5 kit (Zymo Research, Irvine, CA, USA), diluted to a concentration of 10 to 20 nanogram per uL, and sequenced using Illumina MiSeq platform at the Research Technology Support Facility (RTSF) Genomics Core, Michigan State University sequencing facility.

Sequence reads were processed using the OBItools software package (Boyer et al., 2016b; http://metabarcoding.org/obitools) with a few modifications. First, forward and reverse reads were aligned and assembled using *illuminapairedend* and sequences with alignment quality scores < 40 were filtered out. Retained reads were then assigned to relevant samples using the *ngsfilter* tool with allowed primer mismatches of 3 bp and no mismatches allowed in the barcodes. Identical sequences were merged using *obiuniq*. Using *obigrep*, all sequences with only a single copy or shorter than 10 bp were filtered from the data. *Obiclean* was used to identify amplification and sequencing errors. The read trimming was further confirmed by trimming any bases that did not align to NCBI's nucleotide database with BLASTN (task set to "blastn-short" and low-complexity filtering turned off).

Taxonomic assignment of sequences was performed with a local taxonomic reference library containing arctic and boreal vascular and bryophyte taxa (Alsos et al., 2016), after checking that reference taxa were consistent with the NCBI taxonomy scheme (accessed February 2019). Reads were aligned with blastn to the reference database (parameters as described above) and the lowest common ancestor of all matches with an edit distance of two or less was assigned as the read taxonomy. Edit

298 distance was calculated as the sum of alignment gaps, alignment mismatches, and unaligned bases of
299 the read, and was used instead of a relative measure (such as percent identity) because *trn*L intron
300 sequences vary greatly in length (Boyer et al., 2016a).
301 Because of the large variation of values found for individual taxa we combined these data into
302 families for a CONISS-based cluster analysis using Tilia in the same manner as with the morphological
303 macrofossil analysis (v 2.6.1; Grimm, 1987). We defined the transition between bog and permafrost
304 plateau vegetation using this sequence data as the depth at which the CONISS analysis first divided the
305 data into different hierarchies, or clusters within the dendrogram.

306 **3.0f Results**

307 *3.1 ^{210}Pb and ^{7}Be results*

308 We found that ^{210}Pb age estimates for many of the soil horizons were younger than ^{14}C-based dates
309 (Table S1). We also found movement of ^{7}Be as deep as 7 cm (Figure S1), suggesting that there was
310 downwash of both ^{7}Be and ^{210}Pb into the soil profile. This result is supported by the fact that we also
311 found unsupported ^{210}Pb activity as deep as 75 to 135 cm within the soil profile (Manies et al., 2021).
312 Downwash biases the mean accumulation rate (MAR) towards higher values which, in turn, results in
313 younger estimated ages at a specific horizon. Attempts to account for the effect of downwash on ^{210}Pb
314 age dating using two different models was unsuccessful (Manies et al., 2016). Therefore, we did not use
315 ^{210}Pb data in our age models, but instead only use ^{14}C measurements of macrofossils for age modeling.

316 *3.2 Site history*

317 Age model results from the nine cores, all located within the 0.2 km^2 study area, reveal that the onset of
318 peat formation began at the study site between -700 to 500 CE (Table 1). Sites closer to the Tanana
319 River are younger by several hundred years (Figure S2), suggesting that, even within this site's small
320 footprint, peat formation was influenced by the retreat of the river. Plant macrofossils indicate that peat

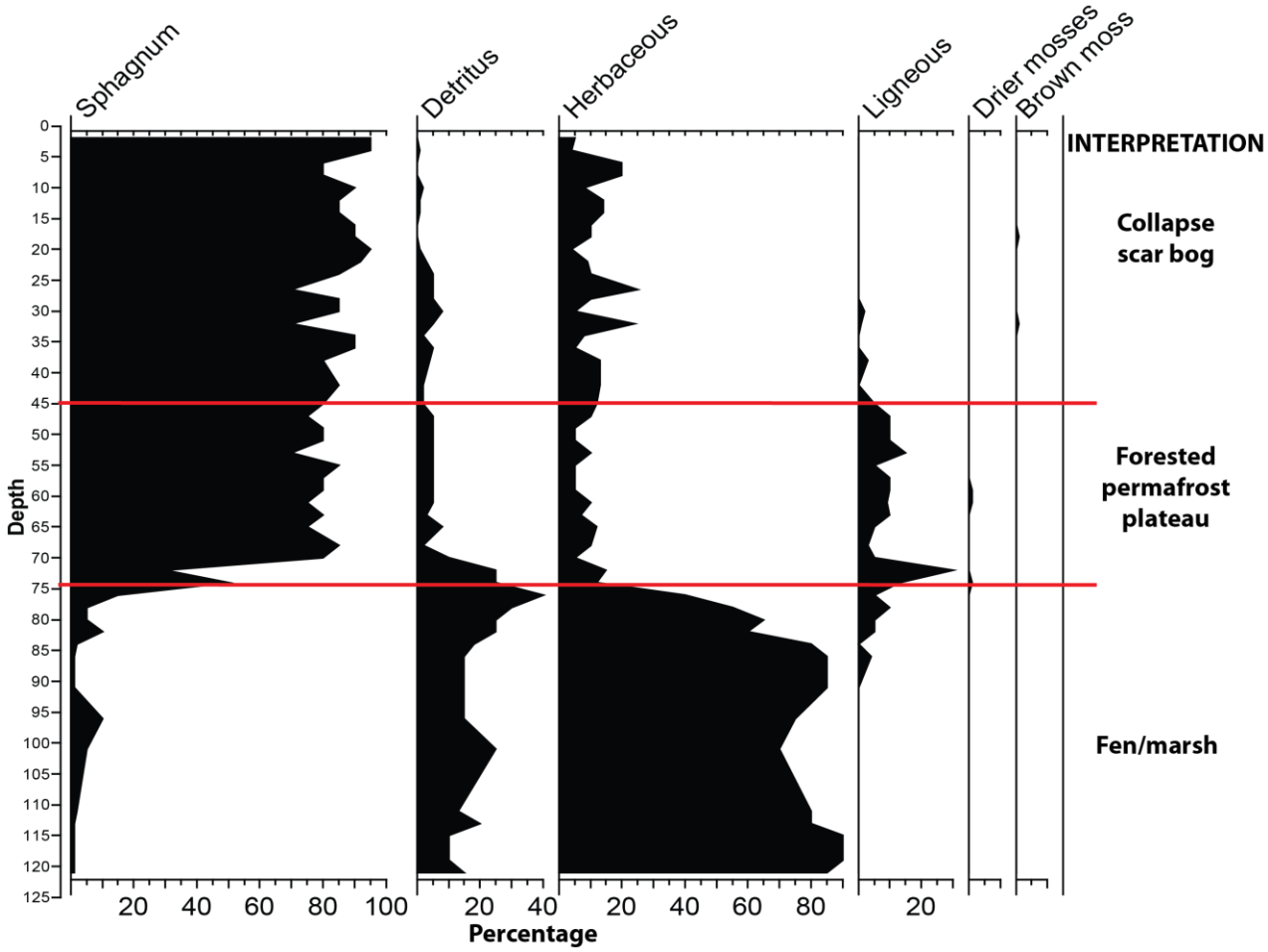

Figure 2. *Simplified macrofossil diagram showing how changes in different amounts of material were used to determine the transitions between stratum ecosystems. Collapse scar bogs were dominated by bryophytic peat, while permafrost plateau forests had high levels of ligneous peat. At the base of all cores was material dominated by herbaceous peat from the initial fen/marsh period. This diagram is for the Young bog-4 core (BB4). Full macrofossil diagrams can be found in Figure S7.*

is dominated by herbaceous material, typically from sedges (Cyperaceae) and ericaceous plants (Figures 2 & S7), indicating that this site was initially dominated by fen and marsh vegetation. Much of the peat within the fen-marsh stratum was classified as plant detritus, indicating this peat's C is highly processed. This marsh/fen stratum was present at the base of all cores.

Above the marsh/fen stratum, all cores transitioned to plant macrofossils dominated by ligneous peat (e.g., black spruce roots or needles, ericaceous shrub roots, leaves; Figures 2 & S7). The transition between herbaceous and ligneous peat indicates when permafrost first aggraded at the site, approx.

1450 - 1770 CE. Cores from the collapse-scar bog also had a surficial stratum dominated by bryophytic peat (*Sphagnum*-dominated, with occasional appearance of brown mosses and Cyperaceae) consistent with permafrost thaw (Figures 2 & S7). Age models suggest that permafrost thaw began between 1874 – 1963 CE (Table 1). Because cores were taken in different locations within each feature (e.g., center and edge) we can use these data to understand how these features expanded. Thaw dates suggest that small features initially formed and that these features expanded in the past decades (Figure S3). To understand more about this expansion, we examined images of the area from 1969 (Declassified CORONA Satellite Imagery) and 1994 (air photos). These images confirm that features were mostly formed by 1969 with slight expansion up to 1994 and present day.

3.3 Macrofossil – DNA comparison

Similar to macrofossils, the relative abundance of the chloroplast nucleic acid biomarker (*trnL*) showed changes in vegetation composition with depth for all cores. Some of the main vegetation classes found in the DNA data align with macrofossils found in relatively high abundance (for example, Betulaceae, Cyperaceae, and Ericaceae). However, even though mosses, especially *Sphagnum* spp., were often a large component of the macrofossil data, none of the moss species identified in the macrofossils were

Site	Core	Peat initiation (CE)	Age of Permafrost aggradation (CE)	Age of Permafrost thaw (CE)
Young bog	BZBB 2	-110 (-226 – 34)	1447 (1285 – 1577)	1933 (1825 – 1971)
	BZBB 3	-203 (-607 – 118)	1469 (1139 – 1671)	1999 (1983 – 2011)
	BZBB 4	-468 (-668 – -376)	1710 (1676 – 1767)	1936 (1868 – 1976)
Intermediate bog	BZBT 1	42 (-50 – 196)	1601 (1475 – 1766)	1954 (1752 – 1981)
	BZBT 9	494 (144 – 952)	1769 (1689 – 1855)	1976 (1969 – 1986)
Old bog	BZSE 3	-49 (-514 – 408)	1563 (1402 – 1756)	1994 (1981 – 2004)
	BZSE 4	-156 (-195 – -100)	1710 (1541 – 1746)	1874 (1705 – 1846)
Permafrost plateau	BZPP 11	84 (-478 – 464)	1623 (1473 – 1769)	--
	BZGC 11	-711 (-910 – -508)	1675 (1464 - 1808)	--

Table 1. *Estimates of ages for peat formation (aka landform age), permafrost aggradation, and permafrost thaw. Age estimates are based on Bacon age model results (Figure S8) using radiocarbon data (Table S2) for the depths at which transitions between stratums were noted using macrofossils (Figure S7).*

identified in the extracted and sequenced DNA. Missing vegetation in DNA analyses, mostly arboreal and *Sphagnum* species, has also been noted by others (Birks & Birks, 2016; Zimmermann et al., 2017). These missing taxa may be due to issues of primer bias, DNA degradation, plant protection of DNA, database representation, and/or DNA extraction efficiency (Parducci et al., 2015). We used the CONISS method (Grimm, 1987), a stratigraphically constrained cluster analysis, to determine where the DNA-based data transitioned from a forested permafrost plateau to a collapse scar bog and compared these values to the macrofossil-based depths. Of the four cores for which we have both *trnL* DNA and morphological-

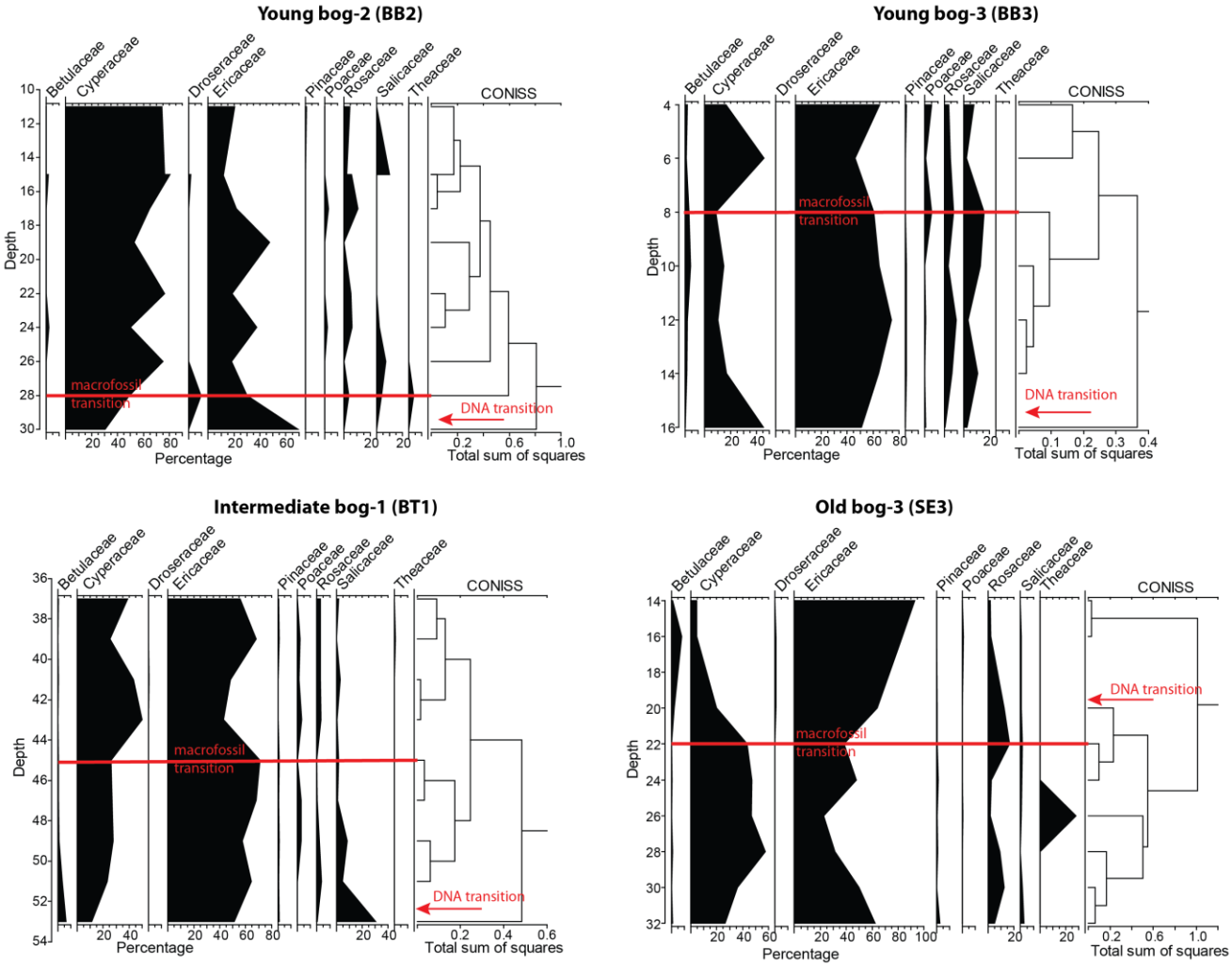

Figure 3. *Vegetation transition analysis from peat cores using CONISS analysis of plant DNA at the family level. The red lines indicate the depths of macrofossil-based strata transitions, while the red arrows indicate where the CONISS analyses indicates the first break in the DNA data.*

364 macrofossil data, two of the DNA dendrograms showed a first-level split into clusters at a similar depth
365 as the macrofossils (Figure 3, Young bog-2 and Old bog-3). In the other two cores the DNA-based depth
366 of transition did not match the macrofossil-based depth (Young bog-3 and Intermediate bog-1). If we
367 relied on the DNA-based first level split the differences in transition depths would have changed the
368 estimated C stocks in the thawed bog stratum -3.2 to 0.5 kg m^{-2}, which is up to a 30 % difference.
369 Because the main identifier of collapse-scar bog peat is the presence of moss species like *Sphagnum*
370 *angustifolium* and *Sphagnum riparium,* we chose to only use the macrofossil approach to determine
371 stratigraphic boundaries.

372 *3.4 C stocks and loss with thaw*

373 Total peat C stocks (to mineral soil) ranged from 24.6 – 93.1 kg m^{-2}, but this C was divided
374 between 2-3 stratums, depending on location of the core. Stocks of C of the fen/marsh stratum ranged
375 between 16 and 42 kg C m^{-2}, with one core having 80 kg C m^{-2} (Table 2). There was a moderate
376 logarithmic relationship between the amount of C within the fen/marsh stratum and the number of
377 years the core was a fen/marsh (a= 2.27, b=-14.65, goodness of fit = 0.49, Figure S4). C stocks for the
378 permafrost forest stratum ranged between 4.6 and 13.0 kg C m^{-2} (Table 2) and also had a moderate

Site	**Core**	**Carbon stocks (kg C m^{-2}) in peat**			
		fen/marsh	**forested permafrost plateau**	**collapse-scar bog**	**Total stocks**
Young bog	BZBB 2	16.4	12.2	3.0	31.7
	BZBB 3	42.4	12.6	0.7	55.6
	BZBB 4	22.2	7.0	9.7	38.9
Intermediate bog	BZBT 1	29.0	4.6	7.4	41.0
	BZBT 9	26.4	11.4	4.9	42.7
Old bog	BZSE 3	17.5	5.5	1.5	24.6
	BZSE 4	22.0	5.5	10.7	38.2
Permafrost plateau	BZPP 11	26.5	12.0	--	38.5
	BZGC 11	80.1	13.0	--	93.1

379 **Table 2.** *C storage (kg m^{-2}) for the three different core strata (fen/marsh, forested permafrost plateau,*
380 *and collapse-scar bog peat) representing the three different periods this site has experienced (post-*
381 *floodplain vegetation, permafrost aggradation, and post-thaw). The permafrost plateau does not have*
382 *bog peat because these areas still contain permafrost.*

logarithmic relationship between C stocks and number of years with permafrost (a=0.7575, b=4.96, goodness of fit = 0.69, Figure S4).

When C loss due to thaw was examined using normalized stocks, we found a loss of C in the century following permafrost thaw of 34%, or 20 kg m^{-2}, with a range of 8 - 60% (95% confidence intervals: Figure 4A). When using the slope method to compare C stocks of cores from the permafrost plateau, where the peat remains frozen, to the non-bog peat for cores where permafrost has thawed (Figure 4B), we find a 46% decrease in C (Figure 4B), which, if peat has accumulated for 2000 years,

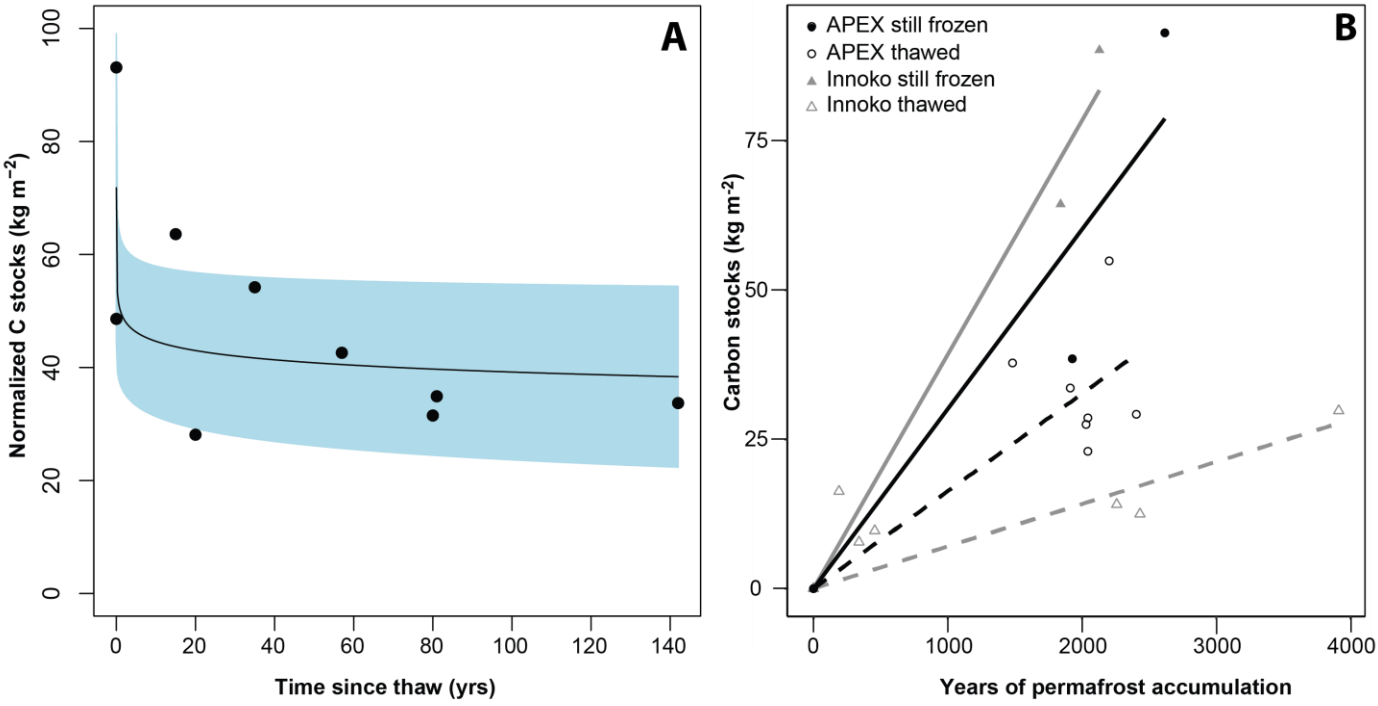

Figure 4. *Estimating carbon losses from APEX permafrost using two methods. A) The Normalized C method, where C stocks were normalized to the oldest core and then plotted against the number of years each core has been thawed (see methods). This method shows a 34% loss of C with time. B) The linear method comparing stocks between still frozen peat (solid lines) and thawed peat (dashed lines) for both the APEX site (black, this study) and Innoko, AK (gray, Jones et al., 2017). With C loss, the slope of the line representing thawed cores (dashed line) will have a lower slope than the slope of the line where the cores still contain permafrost (solid line). Using this method AEPX C losses are estimated at 46% of the existing stocks, but lower than losses of C found for Innoko.*

means a C loss of 27 kg C m^{-2}. If we compare results of the linear method for APEX to those of Innoko, AK, which is of a similar age but formed permafrost syngenetically with peat accumulation (Jones et al., 2017; Figure 4B), we observe both lower C accumulation in APEX than Innoko as well as smaller losses. Thus, C losses (kg m^{-2}) at APEX are over 50% less than found at Innoko. The slope method has two assumptions: 1) peat C at initiation is zero, and 2) peat accumulates linearly with time. A linear relationship may not be a true representation of peat accumulation but the short time span between permafrost initiation and thaw at APEX precludes us from determining the nature of this relationship (i.e., logarithmic, exponential, etc.) Stocks of post-thaw collapse-scar bog peat ranged between 0.7 and 10.7 kgC m^{-2}. While we found a moderate logarithmic relationship between the amount of C and the number of years for which the core was a collapse-scar bog (goodness of fit = 0.60, Figure S4), the initial accumulation rates for this model were unreasonable (>3 kg m^{-2} yr^{-1}). Therefore, a polynomial relationship appears to better represent our data (intercept = -0.1551, x = 0.1996, x^2 = -0.0003, adjusted r^2 = 0.64).

We calculated net C gains/losses by summing C gains with post-thaw moss peat growth (Figure S4) with losses with thaw, using logarithmic relationships for permafrost C loss with thaw (Figure 4A). Results suggest that the site experienced net C losses in the first 10 years following thaw, but post-thaw peat accumulation resulted in net C gains thereafter (Figure 5). Carbon stocks reached their pre-thaw levels within 150 years, regardless of the number of years we model for pre-thaw peat accumulation (Figure 5).

3.5 C:N ratio comparison between APEX and Innoko

C:N ratios can be indicative of how decomposed plant residues are, as C:N ratios typically decline during the decomposition processes, especially when examined with a vegetation type or ecosystem type

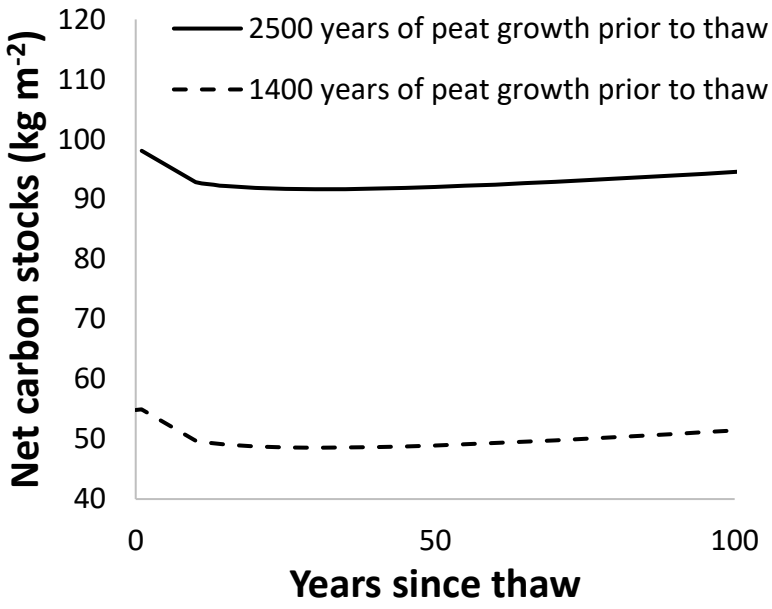

Figure 5. *Net C stocks, modeled as inputs from bog C and losses due to permafrost thaw for two time periods, which represent the upper and lower estimates of that at which peat initiated.*

(Treat et al., 2016). Syngenetic permafrost would, therefore, be expected to have higher C:N ratios than quasi-syngenetic or epigenetic permafrost because in syngenetic permafrost the plant tissue was entrained in permafrost before much decomposition could occur. In contrast, quasi-syngenetic permafrost and epigenetic permafrost forms after peat formation, incorporating peat that has already been exposed to microbial processing. To determine how well nutrient concentrations work in this capacity we compared the C:N ratios, as well as concentrations of C and N, from APEX, which contains quasi-syngenetic permafrost, to Alaskan sites with syngenetic permafrost peat (Innoko and Koyukuk NWR; Jones et al., 2017). An ANOVA (*aov* command; R Core Team, 2017) was used to compare these values between sites and among organic soil horizons. The soil horizons (fibric, mesic, and humic) (Manies et al., 2020) are based on visual quantifications of the degree of decomposition within the soil sample, not a detailed macrofossil analysis. We found that permafrost type ($p < 0.001$, $F = 62.16$), but not horizon code nor a permafrost by horizon code interaction, had a significant effect on C:N ratios. Subsequent statistical comparison of C found similar results, with permafrost type being the only

significant factor ($p < 0.001$, $F = 88.3$), with epigenetic permafrost having lower C concentrations than syngenetic permafrost (31.3 versus 41.2% C, respectively, Figure S6). Permafrost type was also a significant factor for N concentrations ($p < 0.001$, $F = 19.0$), with epigenetic permafrost having higher N than syngenetic permafrost (1.6 versus 1.3 % N, respectively, Figure S6). In addition, there was a permafrost by horizon interaction ($p < 0.03$, $F = 4.7$), with mesic epigenetic permafrost having higher N concentration that humic epigenetic permafrost (1.8 versus 1.3 % N, respectively, Figure S6).

4.0 Discussion

4.1 Site history

The Alaska Peatland Experiment (APEX) research site experienced permafrost thaw within the last half century, resulting in the formation of multiple thermokarst bogs of different ages. The paleoecological history of the site has been influenced local flooding due to its proximity to the Tanana River. Large floods occurred along the Tanana River from -1050 to -50 CE (Mason & Begét, 1991), which coincides with the timing of peat initiation at this site (-710 to - 500 CE; Figure S2), suggesting that a combination of a decrease in river flooding and a movement of the river away from the study site allowed for peat initiation to begin. Variability in peat initiation ages is likely related to differences in local microtopography and hydrology as the Tanana River moved away from the site, with locations to the north and the west of the site (e.g., BZGC11) initiating before areas to the south or east (Figure S2). Macrofossils reveal that these sites existed as permafrost-free fens until permafrost aggraded between 1450 – 1775 CE (Table 1), which corresponds to one of the maxima of the Little Ice Age (LIA; Miller et al., 2012). This timing is also consistent with broader scale Holocene climatic changes that resulted in a general increase in the aggradation of permafrost in northern peatlands ~1000 years ago, culminating during the LIA (Treat & Jones, 2018).

We were surprised to find that the age of permafrost thaw did not correlate to thaw feature size. While thaw in the 'old bog' appears to have begun thawing decades before the two younger bogs, the features we called 'young' and 'intermediate' appear to have begun thawing around the same time (Table 1). What differs between these two bogs is how fast the feature expanded; the young bog remained small for decades and only recently has begun expanding, while the intermediate bog appears to have been expanding since thaw began in the 1950's.

Several reasons could explain the difference in how fast these bogs expanded. One factor could be differences in ice content, as permafrost with high ice content is at greater risk of thaw resulting in thermokarst (Olefeldt et al., 2016; Shur & Jorgenson, 2007). High ice content soil is often associated with fine-grained surficial deposits (Jorgenson & Osterkamp, 2005). The proximity of the APEX site to the Tanana River suggests that, as the river meandered away, areas that were located in low-energy environments could have received higher amounts fine-grained sediment and, thus, could have higher mineral soil ice content. These localized areas of greater ground ice content could cause differential rates of bog expansion upon thaw. To investigate this hypothesis, we examined the volumetric water content (VWC), which would be higher in soils with more ice, of mineral soils below the active layer for cores taken around the site. The VWC content of cores taken near to the young thaw feature was lower ($p = 0.006$, Figure S5) than cores taken near the intermediate thaw feature, which experienced much quicker expansion (VWC 57.3 ± 11.4 % versus 64.6 ± 15.6 %, respectively, mean ± s.d.).

Another factor that could have impacted the rates at which the young and intermediate bogs expanded is soil temperature. Data from Waldrop et al. (2021) show that in September 2015 the deep peat at the intermediate bog was warmer the deep peat at the young bog. Neumann et al. (2019) demonstrated that the temperature of rain and any resulting subsurface flow can impact deep soil temperatures, especially at bog edges. Therefore, if the intermediate bog received more water inputs from the surrounding forested permafrost plateau than the young bog these additional inputs could

have resulted in warmer peat temperatures, which in turn could have expanded the intermediate bog faster than the young bog. Macrofossils support this hypothesis, as cores from the intermediate bog show the presence of brown mosses, which suggests more mineral/nutrient input, such as through groundwater or overland flow. These mosses were not found in the cores from the young bog.

External factors, such as wildfire and solar based thermal inputs could also explain the expansion differences between the young and intermediate bogs. The only core for which charcoal appears in horizons dated from the past two centuries (when thaw began in this area) is Young bog-4. Therefore, although it is possible that fire played a role in advancing permafrost thaw at these bogs, it is not likely. Although the features are surrounded by similar vegetation, local differences in shading at the areas of initial thaw between the young and intermediate bog could have impacted thaw rates. However, ice content and/or water inputs likely played a larger role in these different rates of growth.

4.2 Plant DNA-based stratigraphy

Many studies have demonstrated that DNA-based analyses, such as sequencing of the *trnL* chloroplast intron, can be used to understand long-term paleoecological changes in vegetation similar to macrofossils (i.e. thousands of years; Parducci et al., 2017; Parducci et al., 2015; Zimmermann et al., 2017). Our DNA-based reconstruction identified fewer taxa than identified by the macrofossil analysis, as is consistent with the literature (see Figure 2 of Parducci et al., 2015). Changes in moss species is a key indicator of thaw, both in the field and in macrofossil analyses, but was mostly absent from our DNA analyses. We identified three potential reasons for this under-representation of bryophytes in the sequence-based data set. Firstly, the primers used targeted the P6-loop of the chloroplast *trnL* (UAA) intron, which is a universal, short, plant-specific biomarker. Although these same primers have been shown to successfully amplify and identify *Sphagnum* spp. from Arctic sediment cores, *Sphagnum* are not the main target of these primers and, therefore, amplification may be biased against inclusion in a *trnL* sequence-based dataset (Alsos et al., 2016; Zimmermann et al., 2017). Secondly, the identification

of sequences species relies on the completeness of the reference database. We used European arctic/vascular and bryophyte databases, because as yet no Northern American arctic/boreal plant database with the chloroplast *trnL* (UAA) intron exists, which also could have cause bias against identification of locally adapted *Sphagnum* spp. Finally, when *Sphagnum* biomass is buried cell lysis and the presence of secondary metabolites may increase the rate of DNA degradation (Xie & Lou, 2009). We believe with further improvement this method could be more useful for palaeoecological studies of Alaskan flora and, potentially, though inclusion of *Sphagnum* specific primers, useful for identification of vegetation transitions across broad time scales.

We were interested in knowing if these DNA based methods could be used to mark finer-scale (decadal) transitions between vegetation, such as when permafrost thawed and forested peat plateaus transitioned into inundated wetlands, as this determination using macrofossil data is a time- and training-intensive process. Identification of stratigraphic transitions between bogs and forest peat plateaus using the *trnL* amplicon only matched (within 2 cm) morphological identification-based transitions in two of the four cores we examined. We should note that due to time and sample constraints, we only conducted DNA-based analyses on ~20-cm sections of each core, focused on the area where macrofossil data indicated a vegetation community shift occurred. Even considering this constraint, because the *trnL* vegetation reconstructions using the methods detailed herein do not consistently match macrofossil results we feel they are better used as a complementary tool, one that could be used as a 'first pass' in paleoecological studies, in conjunction with morphological macrofossil analyses, or when examining vegetation shifts across an entire core, representing tens of thousands of years of ecosystem change.

4.3 Estimating C losses in millennial aged permafrost

The magnitude of post-thaw C loss of lowland peatlands remains a matter of debate. While some studies have found large permafrost C losses due to permafrost thaw (Jones et al., 2017;

O'Donnell et al., 2012), others show little to no loss, such that any losses can be relatively quickly recouped with post-thaw peat accumulation (Cooper et al., 2017; Estop-Aragonés et al., 2018a; Estop-Aragonés et al., 2018b; Heffernan et al., 2020). We found evidence that between 34 – 46% of the C available at APEX was lost due to thaw (Figure 4). However, the scatter in our dataset was relatively high, suggesting additional replicate cores and/or a chronosequence spanning a greater period of time would help constrain these values. We attribute the high scatter in the APEX dataset to natural landscape variability, the clustering of thaw ages within a few decades of each other, and radiocarbon calibration uncertainty associated with the timing of thaw coinciding with nuclear weapons testing. Additional sources of uncertainty include the fact that some ages were derived from the age model, due to lack of ^{14}C dates at the depth of transition, and the potential of mixing of macrofossil assemblages, which can happen due to edge slumping. Nonetheless, our data suggests that 20 - 27 kg C m^{-2} was lost due to thaw at APEX (normalized versus linear method, respectively). These values are greater than the 9 kg C m^{-2} of losses found by Heffernan et al. (2020), but less than the 35 – 45 kg C m^{-2} of losses found by Jones et al. (2017). When comparing the APEX data with the data from Innoko, Alaska (Jones et al., 2017), which used similar methods for estimating C loss, we show that the Innoko permafrost plateaus both gained more C prior to thaw and lost more carbon following thaw compared to APEX (Figure 4B). We compared these two sites because peat initiated around the same time (Table 3; Figure 4B). We believe the main difference between these two sites is that Innoko contains syngenetic permafrost, where peat and permafrost accumulation happened simultaneously. In contrast, the permafrost at APEX was classified as quasi-syngenetic permafrost, a form of epigenetic permafrost. Quasi-syngenetic permafrost forms when the permafrost grows upward, like syngenetic permafrost, but incorporates already existing peat/sediments (Kanevskiy, 2003). Therefore, the permafrost at APEX aggraded following peat initiation and has only existed for several hundred years.

555 Differences in permafrost aggradation processes impacts how decomposed peat is, and,
556 therefore, its chemical composition prior to its incorporation into permafrost (Treat et al., 2014).
557 Because syngenetic permafrost is formed when permafrost aggradation and peat accumulation occur in
558 tandem, syngenetic peat is less decomposed and, therefore, likely more susceptible to decomposition
559 upon thaw. In contrast, epigenetic and quasi-epigenetic permafrost are formed with previously
560 deposited sediments/peats, which have already been subject to microbial turnover and, therefore, likely
561 decay more slowly upon thaw. Evidence of high pre-permafrost C processing at APEX is evidenced by an
562 abundance of detrital peat in the fen/marsh stratum (Figures 2 & S6), suggesting that the most labile
563 fraction was processed prior to permafrost aggradation, rendering it less prone to further
564 decomposition upon thaw. This result lies in contrast to the syngenetic permafrost peat plateaus at
565 Innoko and Koyukuk NWR (Alaska), whose peat plateaus contained well-preserved peat in the
566 permafrost (Jones et al., 2017; O'Donnell et al., 2012), subjecting it to rapid decomposition upon thaw.
567 Age factors, such as number of years a site has accumulated peat and had permafrost aggrading,
568 also impact the amount of peat that has accumulated and, thus, the amount of C that can be lost due to
569 thaw. Therefore, we compared these age factors, along with permafrost type, for studies that had
570 examined C loss with permafrost thaw (Table 3). There was no consistent pattern between amount of C
571 lost and landform age. There was also no consistent pattern in number of years for which a site had
572 permafrost and magnitude of C loss. However, there was a trend with higher losses coming from sites
573 with syngenetic permafrost and smaller losses coming from sites with epigenetic or quasi-syngenetic
574 permafrost, suggesting that type of permafrost is an important factor in determining the relative
575 amount of C loss due to thaw. Unfortunately, the one study site that contained both syngenetic and
576 epigenetic permafrost (Estop-Aragonés et al., 2018a) used a different methodology to look at C loss (^{14}C-
577 based methods), precluding an examination into how the presence of both types of permafrost might
578 influence C loss. We also found that, as in other studies (e.g., Heffernan et al., 2020), if losses are

Table 3. *Comparison of common factors for studies that have seen minimal versus large C losses with permafrost thaw. While landform age as well as the number of years the forest peat stratum was frozen and has been thaw all play a role in C loss, another important factor for determining if there will be small versus large losses appears to be permafrost type. Syngenetic permafrost, which consists of relatively unprocessed peat, tends to experience larger C losses, while permafrost that formed after peat formed (epigenetic and quasi-syngenetic), so that the peat has previously been processed, appear to experience small losses.*

Relative amount of C loss	**Permafrost type**	**Landform Initiation**	**Number of years permafrost present**	**Number of years permafrost thawed (approx.)**	**General Location**	**Method**
smaller	epigenetic (processed peat)	-450 – 550 CE (2400 – 1400 BP)	200-400	20 - 100	Fairbanks Alaska[a]	chronosequence
smaller	epigenetic (processed peat)	-6550 CE (8500 BP)	1800	30 – 200	AB, Canada[b, c]	chronosequence, ^{14}C
smaller	syngenetic and epigenetic (unprocessed and processed peat)	-5550 – -4650 CE (6600 – 7500 BP)	Unknown	20 - 130	NWT, Canada[d]	^{14}C
larger	syngenetic (unprocessed peat)	-6050 – -8050 CE (8000 – 1000 BP)	8,000-10,000	30 - 1215	Koyukuk, Alaska[e, f]	chronosequence
larger	syngenetic (unprocessed peat)	-1050 – -50 CE (2000 – 3000 BP)	2,000-3,000	20 - 400	Innoko, Alaska[f]	chronosequence

[a]This study
[b]Heffernan et al. (2020)
[c]Estop-Aragonés et al. (2018b)
[d]Estop-Aragones et al. (2018a), Wolfe et al. (2017)
[e]O'Donnell et al. (2012)
[f]Jones et al. (2017

590 relatively small, they are often recuperated relatively quickly (decades to centuries versus millennia)
591 post-thaw.

592 The role that type of permafrost plays suggests that better understanding of the spatial
593 distribution of syngenetic and epigenetic permafrost could help constrain the landscape-scale
594 magnitude of C loss from permafrost thaw in boreal peat plateaus. While the spatial extent of
595 syngenetic versus epigenetic permafrost is not well documented, analysis of circumpolar peat cores
596 revealed patterns of permafrost aggradation timing relative to peatland age, suggesting that the
597 majority of permafrost peatlands aggraded permafrost epigenetically within the late Holocene and as
598 recently as the Little Ice Age (Treat and Jones, 2018). We must also recognize that soils can reflect
599 complex sequences of different types of permafrost formation, with multiple types of permafrost found
600 within the same location (Kanevskiy et al., 2014; Wolfe et al., 2014).

601 Due to the lack of permafrost type maps and the possibility of both syngenetic and epigenetic
602 permafrost within a single core, other indicators need to be used to determine if thawing peat is
603 susceptible to small or large C losses. Our results suggesting that C:N ratios would be a good first-order
604 indicator of permafrost type align with the results others (Sannel & Kuhry, 2009; Schädel et al., 2014;
605 Treat et al., 2016) In addition, C:N data are more accessible in comparison to macrofossil analyses,
606 which require training and are time intensive. The differences in C:N ratios between permafrost types is
607 driven more by differences in C concentration (epigenetic = 31.3% versus syngenetic = 41.2%; Figure S6)
608 than N concentration (epigenetic = 1.6% versus syngenetic = 1.3%; Figure S6). Epigenetic permafrost
609 also has greater variability in C concentrations than syngenetic permafrost. Lower C concentrations for
610 epigenetic permafrost are representative of the fact that its C has experienced more decomposition
611 (Schädel et al., 2014) than syngenetic permafrost.

5.0 Conclusions

We found that for the APEX site, located near the Tanana River of Interior Alaska, the timing of peat initiation was impacted by proximity to old river channels. Initially these sites were dominated by sedges and woody vegetation, consistent with rich fens that accumulated peat in the absence of permafrost. Permafrost aggraded at this site at the end of the Little Ice Age, consistent with observations of other permafrost peatlands in the discontinuous permafrost zone in Alaska. In the last century, permafrost began to degrade in places, transitioning some of the forested peat plateaus in this area into collapse-scar bogs. We found variable rates of bog expansion for the three different features studied herein and hypothesize that these differences are related to within-site differences such as ground ice content and the amount of overland flow received.

Using two different methods, we found smaller C losses post thaw (20 – 34 kg C m^{-2}) compared to other Alaskan locations. Based on a comparison of our results to other studies in the literature that also examined changes in permafrost C upon thaw, we conclude that in addition to landform age and length of time as permafrost, the permafrost aggradation process influences C loss with thaw. Areas where permafrost aggrades after peat formation (i.e., epigenetic) will experience less C loss with thaw, while sites that have syngenetic permafrost could experience large losses of C with thaw. Therefore, future research into changes in C loss with thaw should include determining the relative coverage of these permafrost types within the boreal region. Where this information is not known C:N ratios can be used to indicate the degree of processing of the peat, informing estimates of the degree of C loss with thaw.

Data Availability

Data used in this study are available from Manies et al. (2021; https://doi.org/10.5066/XXXXXXXX). [Note to reviewers: This data release is currently under internal USGS review, so the doi number has yet to be assigned.]

Acknowledgements

We would like to acknowledge Yen Le for her help with the molecular analyses and Jack McFarland for advice and help efficiently sampling and subsampling these cores. Thanks to Mikhail Kanevskiy for his assistance in determining the type of permafrost found at APEX. We also would like to acknowledge the assistance of the Fairbanks USGS office and the Bonanza Creek LTER, without which this work would not be possible. This work was funded by the USGS Climate and Land Use Change Program. Any use of trade, firm, or product names is for descriptive purposes only and does not imply endorsement by the U.S. Government.

644 **References Cited**
645

646 Alsos, I. G., Sjögren, P., Edwards, M. E., Landvik, J. Y., Gielly, L., Forwick, M., et al. (2016). Sedimentary
647 ancient DNA from Lake Skartjørna, Svalbard: Assessing the resilience of arctic flora to Holocene
648 climate change. *The Holocene, 26*(4), 627-642.
649 Birks, H. J. B., & Birks, H. H. (2016). How have studies of ancient DNA from sediments contributed to the
650 reconstruction of Quaternary floras? *New Phytologist, 209*(2), 499-506.
651 Blaauw, M., & Christen, J. A. (2011). Flexible paleoclimate age-depth models using an autoregressive
652 gamma process. *Bayesian Anal., 6*(3), 457-474.
653 Boyer, F., Mercier, C., Bonin, A., Le Bras, Y., Taberlet, P., & Coissac, E. (2016a). obitools: a unix-inspired
654 software package for DNA metabarcoding. *Mol Ecol Resour, 16*(1), 176-182.
655 Boyer, F., Mercier, C., Bonin, A., Le Bras, Y., Taberlet, P., & Coissac, E. (2016b). obitools: a unix-inspired
656 software package for DNA metabarcoding. *Molecular Ecology Resources, 16*(1), 176-182.
657 Brown, J., Ferrians Jr, O. J., Heginbottom, J. A., & Melnikov, E. S. (1997). *Circum-Arctic map of permafrost*
658 *and ground-ice conditions* Circum-Pacific Map 45.
659 Brown, J., & Kreig, R. A. (1983, July 18-22). *Guidebook to permafrost and related features along the*
660 *Elliott and Dalton highways, Fox to Prudhoe Bay, Alaska.* Paper presented at the Fourth
661 International Conference on Permafrost, University of Alaska, Fairbanks, Alaska.
662 Cooper, M. D. A., Estop-Aragonés, C., Fisher, J. P., Thierry, A., Garnett, M. H., Charman, D. J., et al.
663 (2017). Limited contribution of permafrost carbon to methane release from thawing peatlands.
664 *Nature Climate Change, 7*(7), 507-511.
665 Estop-Aragonés, C., Cooper, M. D. A., Fisher, J. P., Thierry, A., Garnett, M. H., Charman, D. J., et al.
666 (2018a). Limited release of previously-frozen C and increased new peat formation after thaw in
667 permafrost peatlands. *Soil Biology and Biochemistry, 118*, 115-129.
668 Estop-Aragonés, C., Czimczik, C., I., Heffernan, L., Gibson, C., Walker, J., C., Xu, X., & Olefeldt, D. (2018b).
669 Respiration of aged soil carbon during fall in permafrost peatlands enhanced by active layer
670 deepening following wildfire but limited following thermokarst. *Environmental Research Letters,*
671 *13*(8), 085002.
672 Euskirchen, E. S., McGuire, A. D., Chapin, F. S., Yi, S., & Thompson, C. C. (2009). Changes in vegetation in
673 northern Alaska under scenarios of climate change, 2003-2100: implications for climate
674 feedbacks. *Ecological Applications, 19*(4), 1022–1043. doi:10.1890/08-0806.1.
675 Finger, R. A., Turetsky, M. R., Kielland, K., Ruess, R. W., Mack, M. C., & Euskirchen, E. S. (2016). Effects of
676 permafrost thaw on nitrogen availability and plant–soil interactions in a boreal Alaskan lowland.
677 *Journal of Ecology, 104*(6), 1542-1554.
678 Gibson, C., Estop-Aragonés, C., Flannigan, M. D., Thompson, D., & Olefeldt, D. (2019). Increased deep
679 soil respiration detected despite reduced overall respiration in permafrost peat plateaus
680 following wildfire. *Environmental Research Letters, 14*.
681 Greenwell, B. M., & Schubert Kabban, C. M. (2014). investr: An R Packages for Inverse Estimation. *The R*
682 *Journal, 6*, 90-100.
683 Grimm, E. C. (1987). CONISS: a FORTRAN 77 program for stratigraphically constrained cluster analysis by
684 the method of incremental sum of squares. *Computers & Geosciences, 13*(1), 13-35.
685 Harden, J. W., Koven, C. D., Ping, C. L., McGuire, A. D., Camill, P., Jorgenson, M. T., et al. (2012). Field
686 information links permafrost carbon to physical vulnerabilities of thawing. *Geophysical Research*
687 *Letters, 39*(15), L15704.
688 Heffernan, L., Estop-Aragonés, C., Knorr, K.-H., Talbot, J., & Olefeldt, D. (2020). Long-term impacts of
689 permafrost thaw on carbon storage in peatlands: deep losses offset by surficial accumulation.
690 *Journal of Geophysical Research: Biogeosciences, n/a*(n/a), e2019JG005501.

691 Hinzman, L. D., Viereck, L. A., Adams, P. C., Romanovksy, v., & Yoshikawa, K. (2006). Climate and
692 permafrost dynamics of the Alaskan boreal forest. In F. S. Chapin, III, M. W. Oswood, K. Van
693 Cleve, L. A. Viereck, & D. Verbyla (Eds.), *Alaska's Changing Boreal Forest* (pp. 39-61). Oxford,
694 United Kingdom: Oxford University Press.
695 Hugelius, G., Loisel, J., Chadburn, S., Jackson, R. B., Jones, M., MacDonald, G., et al. (2020). Large stocks
696 of peatland carbon and nitrogen are vulnerable to permafrost thaw. *Proceedings of the National*
697 *Academy of Sciences*, 201916387.
698 Jackson, R. B., Lajtha, K., Crow, S. E., Hugelius, G., Kramer, M. G., & Piñeiro, G. (2017). The Ecology of Soil
699 Carbon: Pools, Vulnerabilities, and Biotic and Abiotic Controls. *Annual Review of Ecology,*
700 *Evolution, and Systematics, 48*(1), 419-445.
701 Jones, M., Harden, J., O'Donnell, J., Manies, K., Jorgenson, T., Treat, C., & Ewing, S. (2017). Rapid carbon
702 loss and slow recovery following permafrost thaw in boreal peatlands. *Global Change Biology,*
703 *23*(3), 1109-1127.
704 Jorgenson, M. T., & Osterkamp, T. E. (2005). Response of boreal ecosystems to varying modes of
705 permafrost degradation. *Canadian Journal of Forest Research, 35*(9), 2100-2111.
706 Jungqvist, G., Oni, S. K., Teutschbein, C., & Futter, M. N. (2014). Effect of Climate Change on Soil
707 Temperature in Swedish Boreal Forests. *PLoS ONE, 9*(4).
708 Kanevskiy, M. (2003). *Cryogenetic structure of mountain slope deposits, northeast Russia.* Paper
709 presented at the 8th International Conference on Permafrost, Zurich, Switzerland.
710 Kanevskiy, M., Jorgenson, T., Shur, Y., O'Donnell, J. A., Harden, J. W., Zhuang, Q., & Fortier, D. (2014).
711 Cryostratigraphy and Permafrost Evolution in the Lacustrine Lowlands of West-Central Alaska.
712 *Permafrost and Periglacial Processes, 25*(1), 14-34.
713 Leewis, M.-C., Berlemont, R., Podgorski, D. C., Srinivas, A., Zito, P., Spencer, R. G. M., et al. (2020). Life at
714 the Frozen Limit: Microbial Carbon Metabolism Across a Late Pleistocene Permafrost
715 Chronosequence. *Frontiers in Microbiology, 11*(1753). Original Research.
716 Malmer, N., Albinsson, C., Svensson, B. M., & Wallén, B. (2003). Interferences between Sphagnum and
717 vascular plants: effects on plant community structure and peat formation. *Oikos, 100*(3), 469-
718 482.
719 Manies, K., Waldrop, M., & Harden, J. (2020). Generalized models to estimate carbon and nitrogen
720 stocks of organic soil horizons in Interior Alaska. *Earth Syst. Sci. Data, 12*(3), 1745-1757.
721 Manies, K. L., Fuller, C., & Jones, M. (2016). *Modeling Peat Ages Using ^{7}Be Data to Account for*
722 *Downwash of ^{210}Pb*. Paper presented at the American Geophysical Union Fall Meeting, San
723 Francisco, CA. https://ui.adsabs.harvard.edu/abs/2016AGUFM.B23C0597M
724 Manies, K. L., Fuller, C. C., Jones, M. C., Waldrop, M. P., & McGeehin, J. P. (2017). *Soil data for a*
725 *thermokarst bog and the surrounding permafrost plateau forest, located at Bonanza Creek Long*
726 *Term Ecological Research Site, Interior Alaska* Open-File Report 2016-1173.
727 Manies, K. L., Jones, M. C., Waldrop, M. P., Leewis, M.-C., Hoefke, K., Fuller, C., & Cornman, R. S. (2021).
728 *Soil data and age models used to investigate the effects of permafrost thaw on carbon storage,*
729 *Interior Alaska*.
730 Mason, O. K., & Begét, J. E. (1991). Late Holocene flood history of the Tanana River, Alaska, USA. *Arctic*
731 *and Alpine Research, 23*(4), 392-403.
732 Miller, G. H., Geirsdóttir, Á., Zhong, Y., Larsen, D. J., Otto-Bliesner, B. L., Holland, M. M., et al. (2012).
733 Abrupt onset of the Little Ice Age triggered by volcanism and sustained by sea-ice/ocean
734 feedbacks. *Geophysical Research Letters, 39*(2).
735 Neumann, R. B., Moorberg, C. J., Lundquist, J. D., Turner, J. C., Waldrop, M. P., McFarland, J. W., et al.
736 (2019). Warming effects of spring rainfall increase methane emissions from thawing permafrost.
737 *Geophysical Research Letters, 46*, 1393-1401.

O'Donnell, J. A., Jorgenson, M. T., Harden, J. W., McGuire, A. D., Kanevskiy, M., & Wickland, K. P. (2012). The effects of permafrost thaw on soil hydrologic, thermal, and carbon dynamics in an Alaskan peatland. *Ecosystems, 15*, 213-229.

Olefeldt, D., Goswami, S., Grosse, G., Hayes, D., Hugelius, G., Kuhry, P., et al. (2016). Circumpolar distribution and carbon storage of thermokarst landscapes. *Nature Communications, 7*, 13043. Article.

Oliva, M., & Fritz, M. (2018). Permafrost degradation on a warmer Earth: Challenges and perspectives. *Current Opinion in Environmental Science & Health, 5*, 14-18.

Parducci, L., Bennett, K. D., Ficetola, G. F., Alsos, I. G., Suyama, Y., Wood, J. R., & Pedersen, M. W. (2017). Ancient plant DNA in lake sediments. *New Phytologist, 214*(3), 924-942.

Parducci, L., Väliranta, M., Salonen, J. S., Ronkainen, T., Matetovici, I., Fontana, S. L., et al. (2015). Proxy comparison in ancient peat sediments: pollen, macrofossil and plant DNA. *Philosophical Transactions of the Royal Society B: Biological Sciences, 370*(1660), 20130382.

Pella, E. (1990a). Elemental organic analysis. Part 1-Historical developments. *American Laboratory, 22*(2), 116–125.

Pella, E. (1990b). Elemental organic analyzer. Part 2-State of the art. *American Laboratory, 22*(12), 28–32.

R Core Team. (2017). R: A language and environment for statistical computing. Vienna, Austria: R Foundation for Statistical Computing. Retrieved from https://www.R-project.org/.

Rand, J., & Mellor, M. (1985). *Ice-coring augers for shallow depth sampling* CRREL Report 85-21.

Rodenhizer, H., Ledman, J., Mauritz, M., Natali, S. M., Pegoraro, E., Plaza, C., et al. (2020). Carbon Thaw Rate Doubles When Accounting for Subsidence in a Permafrost Warming Experiment. *Journal of Geophysical Research: Biogeosciences, 125*(6), e2019JG005528.

Sannel, A. B. K., & Kuhry, P. (2009). Holocene peat growth and decay dynamics in sub-arctic peat plateaus, west-central Canada. *Boreas: Boreas, 38*(1), 13–24. Article.

Schädel, C., Schuur, E. A. G., Bracho, R., Elberling, B., Knoblauch, C., Lee, H., et al. (2014). Circumpolar assessment of permafrost C quality and its vulnerability over time using long-term incubation data. *Global Change Biology, 20*(2), 641-652.

Schuur, E. A., McGuire, A. D., Schädel, C., Grosse, G., Harden, J. W., Hayes, D. J., et al. (2015). Climate change and the permafrost carbon feedback. *Nature, 520*(7546), 171-179.

Shur, Y., Jorgenson, M. T., & Kanevskiy, M. Z. (2011). Permafrost. In V. P. Singh, P. Singh, & U. K. Haritashya (Eds.), *Encyclopedia of Snow, Ice and Glaciers* (pp. 841-848). Dordrecht: Springer Netherlands.

Shur, Y. L., & Jorgenson, M. T. (2007). Patterns of permafrost formation and degradation in relation to climate and ecosystems. *Permafrost and Periglacial Processes, 18*(1), 7-19.

Soil Survey Staff. (1951). *Soil survey manual* (Vol. Handbook No. 18). Washington, D.C.: Agricultural Research Administration, United States Department of Agriculture.

Taberlet, P., Coissac, E., Pompanon, F., Gielly, L., Miquel, C., Valentini, A., et al. (2006). Power and limitations of the chloroplast trn L (UAA) intron for plant DNA barcoding. *Nucleic Acids Research, 35*(3), e14-e14.

Thormann, M., Szumigalski, A., & Bayley, S. (1999). Aboveground peat and carbon accumulation potentials along a bog-fen-marsh wetland gradient in southern boreal Alberta, Canada. *Wetlands, 19*(2), 305-317.

Treat, C. C., & Jones, M. C. (2018). Near-surface permafrost aggradation in Northern Hemisphere peatlands shows regional and global trends during the past 6000 years. *The Holocene, 28*(6), 998-1010.

Treat, C. C., Jones, M. C., Camill, P., Gallego-Sala, A., Garneau, M., Harden, J. W., et al. (2016). Effects of permafrost aggradation on peat properties as determined from a pan-Arctic synthesis of plant macrofossils. *Journal of Geophysical Research: Biogeosciences, 121*(1), 78-94.

Treat, C. C., Wollheim, W. M., Varner, R. K., Grandy, A. S., Talbot, J., & Frolking, S. (2014). Temperature and peat type control CO_2 and CH_4 production in Alaskan permafrost peats. *Global Change Biology, 20*(8), 2674–2686.

Turetsky, M. R., Kane, E. S., Harden, J. W., Ottmar, R. D., Manies, K. L., Hoy, E., & Kasichke, E. S. (2011). Recent acceleration of biomass burning and carbon losses in Alaskan forests and peatlands. *Nature Geosciences, 4*, 27–31.

Turetsky, M. R., Manning, S. W., & Wieder, R. K. (2004). Dating Recent Peat Deposits. *Wetlands, 24*(2), 324.

Van Metre, P. C., & Fuller, C. C. (2009). Dual-core mass-balance approach for evaluating mercury and ^{210}Pb atmospheric fallout and focusing to lakes. *Environmental Science & Technology, 43*, 26-32.

Waldo, N. B., Hunt, B. K., Fadely, E. C., Moran, J. J., & Neumann, R. B. (2019). Plant root exudates increase methane emissions through direct and indirect pathways. *Biogeochemistry, 145*(1), 213-234.

Waldrop, M. P., McFarland, J., Manies, K., Leewis, M. C., Blazewicz, S. J., Jones, M. C., et al. (2021). Carbon fluxes and microbial activities from boreal peatlands experiencing permafrost thaw. *Journal of Geochemical Research - Biogeosciences*.

Wolfe, S. A., & Morse, P. D. (2017). Lithalsa Formation and Holocene Lake-Level Recession, Great Slave Lowland, Northwest Territories. *Permafrost and Periglacial Processes, 28*(3), 573-579.

Wolfe, S. A., Short, N. H., Morse, P. D., Schwarz, S. H., & Stevens, C. W. (2014). Evaluation of RADARSAT-2 DInSAR Seasonal Surface Displacement in Discontinuous Permafrost Terrain, Yellowknife, Northwest Territories, Canada. *Canadian Journal of Remote Sensing, 40*(6), 406-422.

Xie, C.-F., & Lou, H.-X. (2009). Secondary Metabolites in Bryophytes: An Ecological Aspect. *Chemistry & Biodiversity, 6*(3), 303-312.

Zhang, T., Heginbottom, J., Barry, R., & Brown, J. (2000). Further statistics on the distribution of permafrost and ground ice in the Northern Hemisphere. *Polar Geography, 24*, 126-131.

Zimmermann, H. H., Raschke, E., Epp, L. S., Stoof-Leichsenring, K. R., Schwamborn, G., Schirrmeister, L., et al. (2017). Sedimentary ancient DNA and pollen reveal the composition of plant organic matter in Late Quaternary permafrost sediments of the Buor Khaya Peninsula (north-eastern Siberia). *Biogeosciences, 14*(3), 575-596.

STAND ALONE VERSION OF TABLES AND FIGURES

Site	Core	Peat initiation (CE)	Age of Permafrost aggradation (CE)	Age of Permafrost thaw (CE)
Young bog	BZBB 2	-110 (-226 – 34)	1447 (1285 – 1577)	1933 (1825 – 1971)
	BZBB 3	-203 (-607 – 118)	1469 (1139 – 1671)	1999 (1983 – 2011)
	BZBB 4	-468 (-668 – -376)	1710 (1676 – 1767)	1936 (1868 – 1976)
Intermediate bog	BZBT 1	42 (-50 – 196)	1601 (1475 – 1766)	1954 (1752 – 1981)
	BZBT 9	494 (144 – 952)	1769 (1689 – 1855)	1976 (1969 – 1986)
Old bog	BZSE 3	-49 (-514 – 408)	1563 (1402 – 1756)	1994 (1981 – 2004)
	BZSE 4	-156 (-195 – -100)	1710 (1541 – 1746)	1874 (1705 – 1846)
Permafrost plateau	BZPP 11	84 (-478 – 464)	1623 (1473 – 1769)	--
	BZGC 11	-711 (-910 – -508)	1675 (1464 - 1808)	--

Table 1. *Estimates of ages for peat formation (aka landform age), permafrost aggradation, and permafrost thaw. Age estimates are based on Bacon age model results (Figure S8) using radiocarbon data (Table S2) for the depths at which transitions between stratums were noted using macrofossils (Figure S7).*

Site	Core	Carbon stocks (kg C m^{-2}) in peat			
		fen/marsh	forested permafrost plateau	collapse-scar bog	Total stocks
Young bog	BZBB 2	16.4	12.2	3.0	31.7
	BZBB 3	42.4	12.6	0.7	55.6
	BZBB 4	22.2	7.0	9.7	38.9
Intermediate bog	BZBT 1	29.0	4.6	7.4	41.0
	BZBT 9	26.4	11.4	4.9	42.7
Old bog	BZSE 3	17.5	5.5	1.5	24.6
	BZSE 4	22.0	5.5	10.7	38.2
Permafrost plateau	BZPP 11	26.5	12.0	--	38.5
	BZGC 11	80.1	13.0	--	93.1

Table 2. *C storage (kg m^{-2}) for the three different core strata (fen/marsh, forested permafrost plateau, and collapse-scar bog peat) representing the three different periods this site has experienced (post-floodplain vegetation, permafrost aggradation, and post-thaw). The permafrost plateau does not have bog peat because these areas still contain permafrost.*

Table 3. *Comparison of common factors for studies that have seen minimal versus large C losses with permafrost thaw. While landform age as well as the number of years the forest peat stratum was frozen and has been thaw all play a role in C loss, another important factor for determining if there will be small versus large losses appears to be permafrost type. Syngenetic permafrost, which consists of relatively unprocessed peat, tends to experience larger C losses, while permafrost that formed after peat formed (epigenetic and quasi-syngenetic), so that the peat has previously been processed, appear to experience small losses.*

Relative amount of C loss	**Permafrost type**	**Landform Initiation**	**Number of years permafrost present**	**Number of years permafrost thawed (approx.)**	**General Location**	**Method**
smaller	epigenetic (processed peat)	-450 – 550 CE (2400 – 1400 BP)	200-400	20 - 100	Fairbanks Alaska[a]	chronosequence
smaller	epigenetic (processed peat)	-6550 CE (8500 BP)	1800	30 – 200	AB, Canada[b, c]	chronosequence, ^{14}C
smaller	syngenetic and epigenetic (unprocessed and processed peat)	-5550 – -4650 CE (6600 – 7500 BP)	Unknown	20 - 130	NWT, Canada[d]	^{14}C
larger	syngenetic (unprocessed peat)	-6050 – -8050 CE (8000 – 1000 BP)	8,000-10,000	30 - 1215	Koyukuk, Alaska[e, f]	chronosequence
larger	syngenetic (unprocessed peat)	-1050 – -50 CE (2000 – 3000 BP)	2,000-3,000	20 - 400	Innoko, Alaska[f]	chronosequence

[a]This study
[b]Heffernan et al. (2020)
[c]Estop-Aragonés et al. (2018)
[d]Estop-Aragones et al. (2018a), Wolfe et al. (2017)
[e]O'Donnell et al. (2012)
[f]Jones et al. (2017)

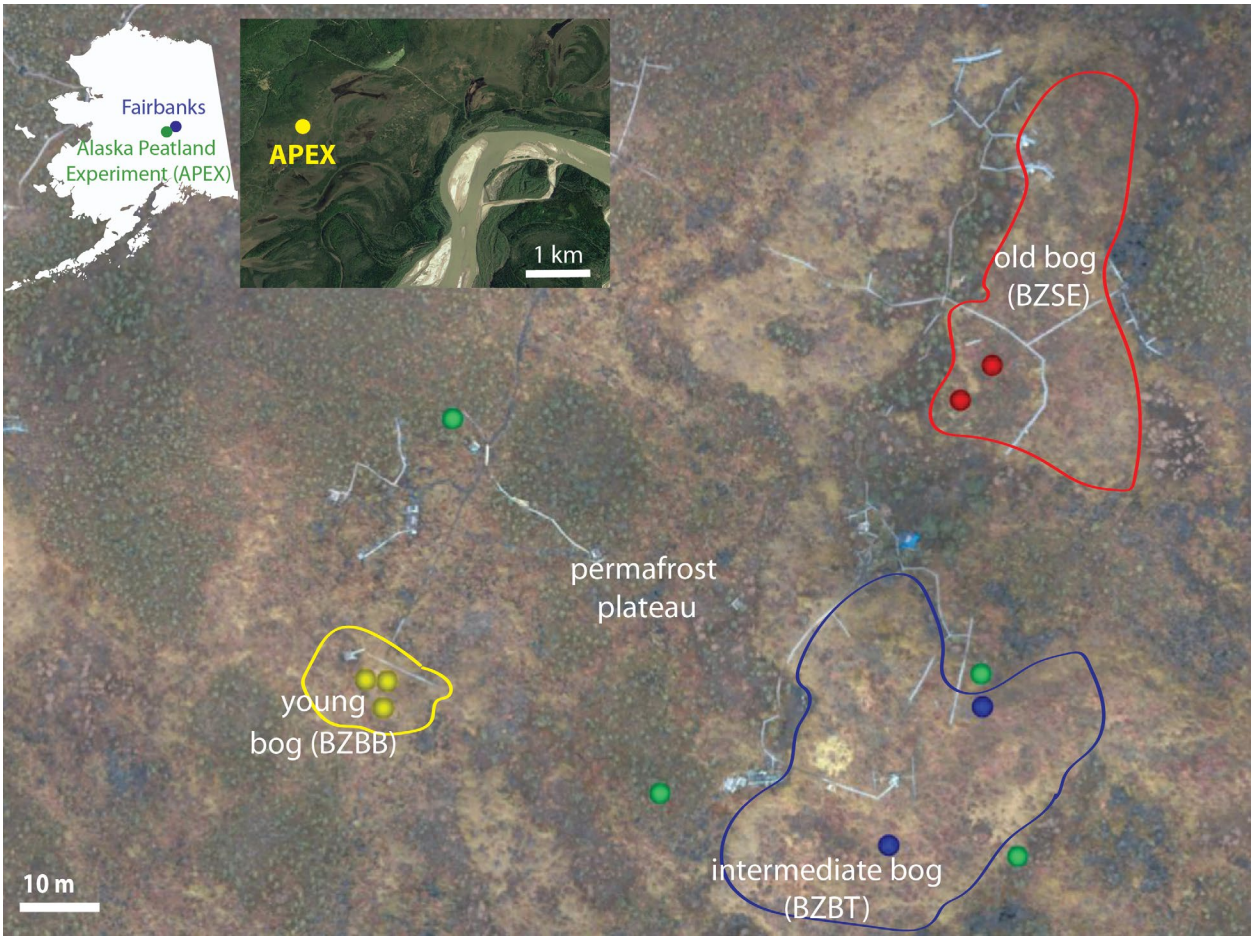

Figure 1. *The Alaskan Peatland Experiment (APEX) site. This area is a mosaic of collapse-scar bogs within forested permafrost plateaus. Colors correspond to the different bogs: the 'old' bog is in red (BZSE), the 'intermediate' bog is in blue (BZBT), and the 'young' bog is in yellow (BZBB). Circles indicate the locations of the soil cores; green circles are cores taken from the permafrost plateau. Core numbers can be found in Figure S2. APEX is located near Fairbanks, close to the Tanana River, in the Interior of Alaska. Images: site - J. Hollingsworth; satellite – Google Earth.*

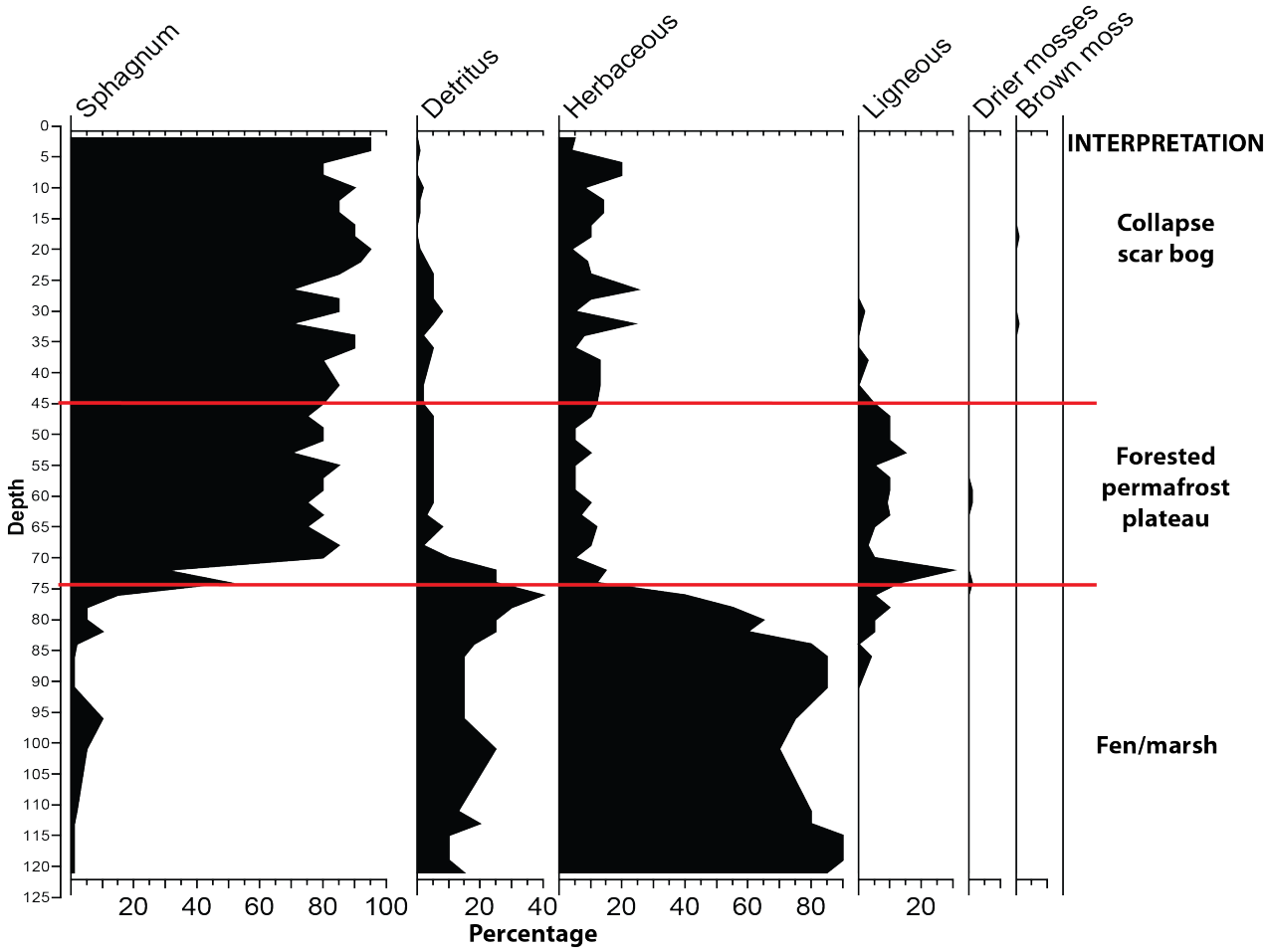

Figure 2. *Simplified macrofossil diagram showing how changes in different amounts of material were used to determine the transitions between stratum ecosystems. Collapse scar bogs were dominated by bryophytic peat, while permafrost plateau forests had high levels of ligneous peat. At the base of all cores was material dominated by herbaceous peat from the initial fen/marsh period. This diagram is for the Young bog-4 core (BB4). Full macrofossil diagrams can be found in Figure S7.*

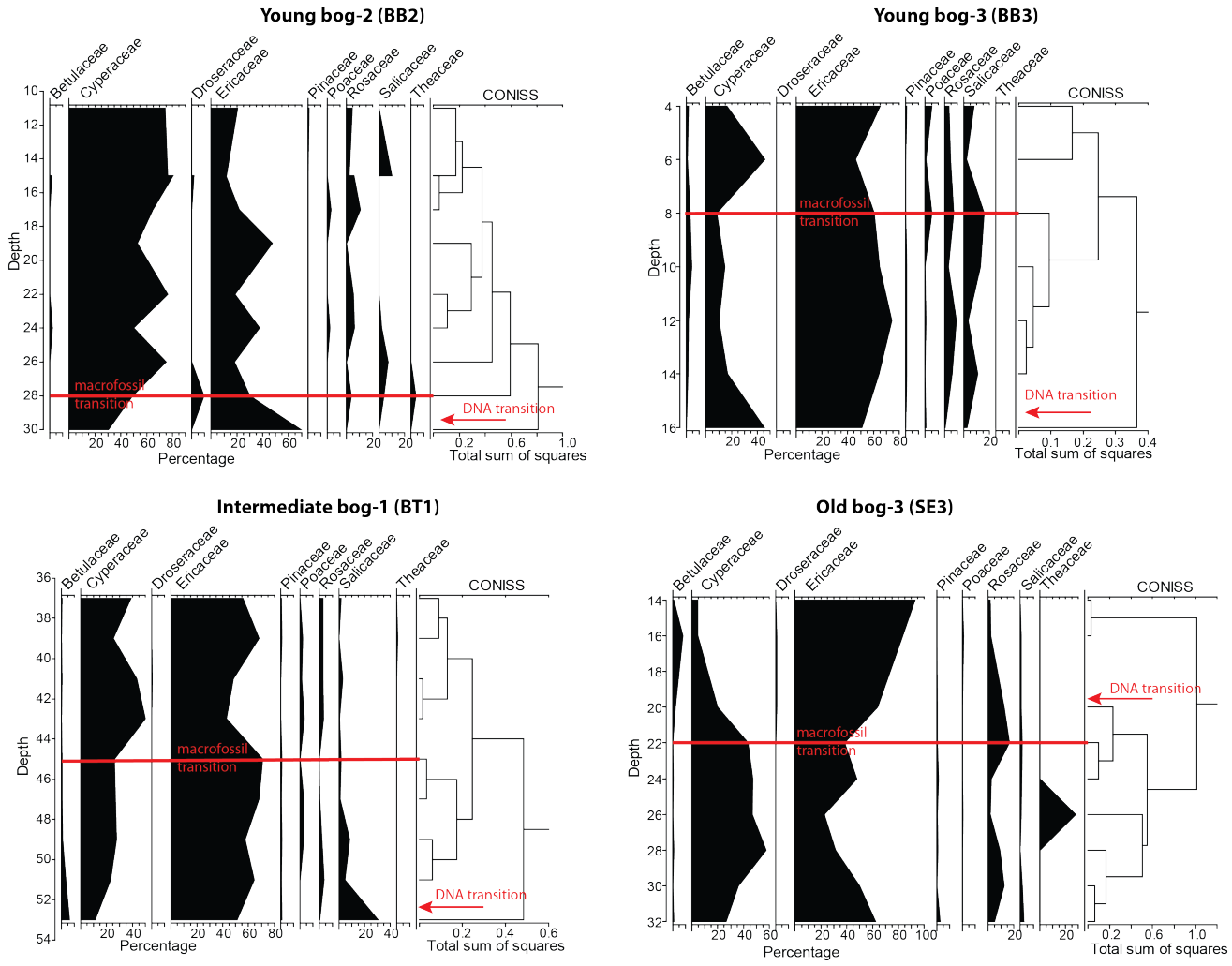

Figure 3. *Vegetation transition analysis from peat cores using CONISS analysis of plant DNA at the family level. The red lines indicate the depths of macrofossil-based strata transitions, while the red arrows indicate where the CONISS analyses indicates the first break in the DNA data.*

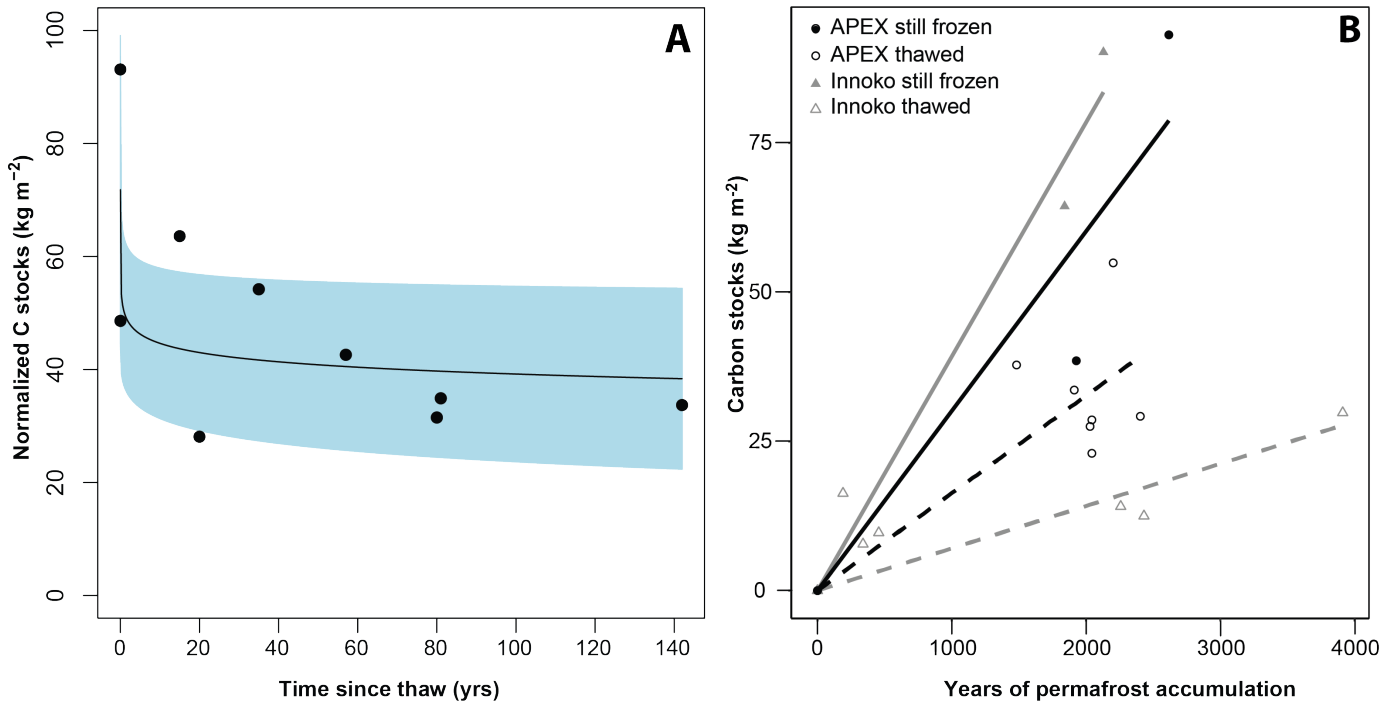

Figure 4. *Estimating carbon losses from APEX permafrost using two methods. A) The Normalized C method, where C stocks were normalized to the oldest core and then plotted against the number of years each core has been thawed (see methods). This method shows a 34% loss of C with time. B) The linear method comparing stocks between still frozen peat (solid lines) and thawed peat (dashed lines) for both the APEX site (black, this study) and Innoko, AK (gray, Jones et al., 2017). With C loss, the slope of the line representing thawed cores (dashed line) will have a lower slope than the slope of the line where the cores still contain permafrost (solid line). Using this method AEPX C losses are estimated at 46% of the existing stocks, but lower than losses of C found for Innoko.*

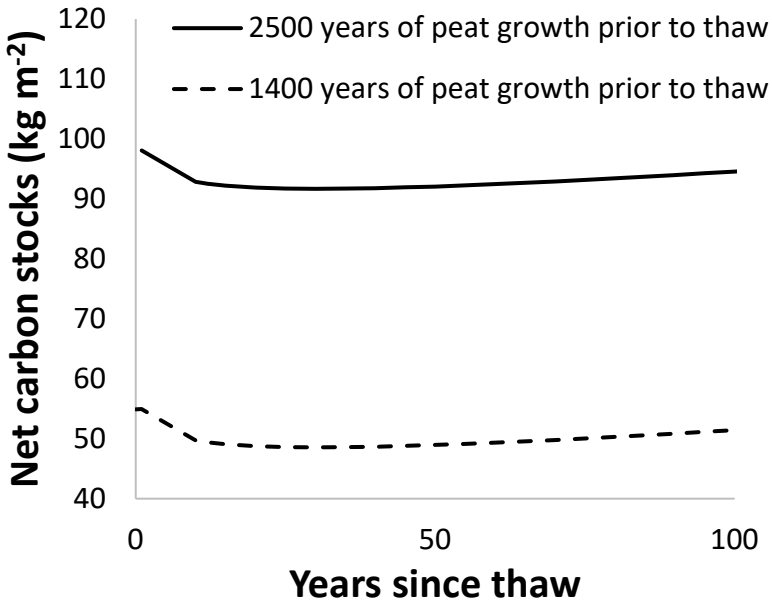

Figure 5. *Net C stocks, modeled as inputs from bog C and losses due to permafrost thaw for two time periods, which represent the upper and lower estimates of that at which peat initiated.*

SUPPLEMENTAL INFORMATION

^{210}Pb and ^{7}Be analysis

^{7}Be, which has similar atmospheric depositional source as ^{210}Pb but a much shorter half-life (53 days vs 22.1 years), was used constrain if there was downward movement of fallout radionuclide bearing particles through our soil profiles over the mean life of ^{7}Be. Four additional surface cores (for measuring ^{7}Be activity) were taken at the Intermediate bog location (BZBT) over a period of ~5 months the summer of 2015 by cutting blocks of peat out of the bog. Each core was divided into horizons, most between 2-5 cm thick, and analyzed for bulk density. We found ^{7}Be down to 7 cm (Figure S1). This depth is similar to, but on the shallow end, for values found within bogs and fens in Sweden (8 - 20 cm; Hansson et al., 2014). Based on our measurements in early May, there does not appear to be large inputs of ^{7}Be in late season snowfall (Figure S1). Early summer rain events were the main source of ^{7}Be (and thus ^{210}Pb) into the soil, transporting ^{7}Be up to 7 cm into the soil. We see penetration of ^{7}Be in August or September only to 4 cm due to the many small rain events during this time, which resulted in lower deposition of ^{7}Be and likely less downward transport into the soil. Because ^{7}Be is a short-lived radionuclide, these data do not provide information about the inputs from earlier in the winter. Attempts to model this downwash affect for ^{210}Pb using two different ages models was not successful (Manies et al, 2016). Therefore, we did not include ^{210}Pb data in our age modeling for our soil cores, instead relying solely on ^{14}C data.

Table S1. A comparison of age estimates using ^{14}C data (either from Calibomb or Calib; see Table S2) and date estimates for base depth of selected core intervals from the CRS model using ^{210}Pb data. The tendency of the ^{210}Pb ages to be younger than ^{14}C ages, in addition to finding ^{210}Pb deep within our soil cores, led us to suspect that ^{210}Pb was mobile in these sites. This hypothesis was confirmed using ^{7}Be (see above text).

Core ID	Depth Range (cm)	Fraction Modern	^{14}C date range (yr)	^{210}Pb date	^{210}Pb error (yrs)	^{210}Pb older or younger than ^{14}C age?
BZBB 2	24-26	1.1040	1996.1– 2000.1	1999.2	1.3	same
BZBB 4	26-28	1.1080	1995.6 – 1999.3	1994.6	2.7	older
	36-38	1.211	1983.9 – 1986.2	1982.5	4.5	older
	72-74	1.0054	1954.9 – 1956.4	1944.1	20.5	older
BZBT 1	32-34	1.2410	1982.0 – 1984.1	1988.8	1.3	younger
	40-45	1.0535	1956.6 – 1957.2	1981.8	3.3	younger
	50-55	0.9864	1802 – 1938	1940.6	33.6	younger
	65-70	0.9521	1439 – 1522	1915.5	42.4	younger
BZBT 9	35-40	1.5671	1968.1 – 1970.1	2001.1	0.5	younger
	47-49	0.9796	1725 - 1787	1999.8	0.6	younger
	80-85	0.9852	1726 - 1814	1974.1	2.3	younger
BZBT 11	31-32	0.9749	1736 - 1805	1912.2	30.0	younger
BZSE 4	42-44	1.003	1954.8 – 1956.0	1942.8	14.0	older
	54-56	0.9758	1619 - 1670	1901.3	108.0	younger

SUPPLEMENTAL INFORMATION

Figure S1. ^{7}Be with depth for four timepoints within the summer of 2015 at the BZBT 1 site. The deeper movement of ^{7}Be within the soil profile may be correlated with the precipitation (A), with sampling events noted by the red lines. The integrated ^{7}Be inventory (B) shows increase over time reflecting ongoing input from atmospheric deposition that exceeds decay of previously deposited ^{7}Be activity.

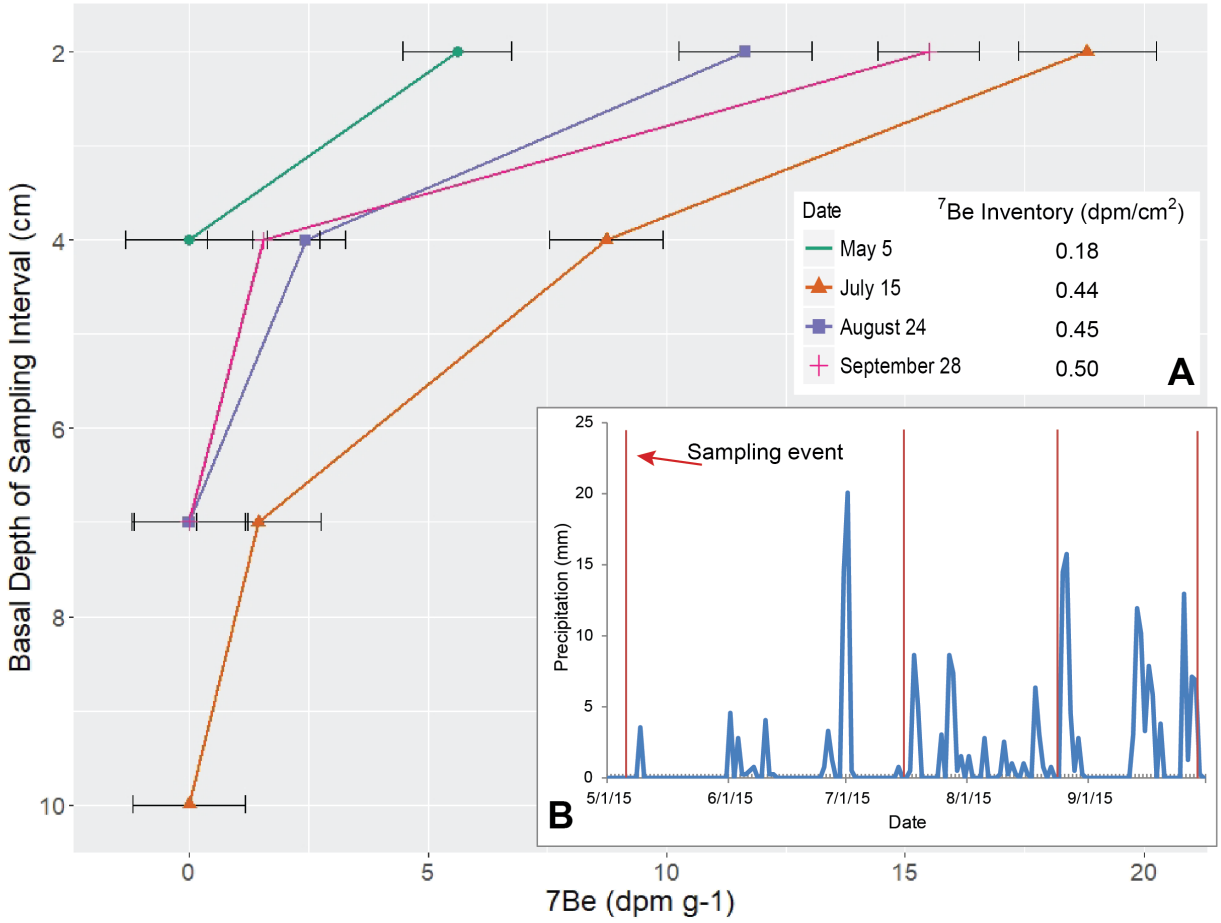

SUPPLEMENTAL INFORMATION

Table S2. Radiocarbon laboratory data. Dates were obtained from three labs: 1) LLNL: samples were prepared and analyzed at the Center for Accelerator Mass Spectrometry (CAMS) at the Lawrence Livermore National Laboratory (LLNL), 2) USGS: sample preparation occurred at the U.S. Geological Survey Radiocarbon Laboratory, while samples were analyzed at the CAMS LLNL, and 3) Beta: samples were prepared and analyzed at Beta Analytic (Miami, FL). Fraction Modern values and errors not given in the data report were calculated using CALIBomb (http://calib.org/CALIBomb/) using intercal13 as the pre-bomb calibration data set and NZ1 as the post-bomb calibration data set. Samples labeled BZBB are from the young bog, BZBT 1 & BZBT 9 are from the intermediate bog, and BZSE are from the old bog. Samples from BZBT 11 and BZGT are from the forest permafrost plateau.

Sample Name	Depth Range (cm)	Description	Lab #	14C age	14C age error	Fraction Modern	Modern error
BZBB 2.26	24-26	*Sphagnum riparium*	LLNL-177606	>modern	-	1.1040	0.0032
BZBB 2.40	39-42	*Vaccinium oxycoccus* leaves, *Picea mariana* needles	Beta-397861	-	-	1.2392	0.0046
BZBB 2.106	103-106	charcoal	LLNL-177605	2125	25	0.7675	0.0022
BZBB 3.14	12-14	*Picea mariana* branchlet	LLNL-177608	>modern	-	1.1815	0.0038
BZBB 3.53	50-53	charcoal	LLNL-177609	115	25	0.9858	0.0028
BZBB 3.80	77-80	charcoal	LLNL-177610	1615	25	0.8179	0.0023
BZBB 3.116+	116 - ~117	charcoal	LLNL-177607	4230	25	0.5906	0.0017
BZBB 4b.28 Suppl	26-28	*Picea mariana* needles, unidentified leaf fragment, *Sphagnum* spp. leaves & stems	Beta-399724	-	-	1.1175	0.0028
BZBB 4b.32	30-32	*Picea mariana* needle, leaf fragment, *Sphagnum* spp. stems	Beta-397863	-	-	1.1217	0.0045
BZBB 4b.38	36-38	*V. oxycoccus* leaves, *Picea mariana* needles, *Sphagnum* spp. stems	Beta-397864	-	-	1.2207	0.0030
BZBB 4.74	72-74	*Sphagnum* spp. stems, shrub leaves	LLNL-177611	modern	-	1.0054	0.0029
BZBB 4.78	76-78	*Sphagnum* spp. stems, charcoal	Beta-415694	200	30	0.98302	0.0036
BZBB 4.121	119-121	charcoal	LLNL-179988	2425	30	0.7395	0.0026
BZBB 4.136	128-136	charcoal	Beta-415693	3540	30	0.6486	0.0024
BZBT 1.33	32-34	Undifferentiated plant material	USGS-9502	>modern	-	1.2410	0.0035
BZBT 1a.45	40-45	*Sphagnum* spp. stems	LLNL-177615	>modern	-	1.0535	0.0030
BZBT 1a.55	50-55	*Vaccinium* spp. leaves	LLNL-177034	110	30	0.9864	0.0035

SUPPLEMENTAL INFORMATION

BZBT 1a.70	65-70	plant material	USGS-9503	395	30	0.9521	0.0031
BZBT 1.117	117-119	charcoal	LLNL-179989	1975	30	0.7819	0.0027
BZBT 1a.122	117-122	charcoal	USGS-9504	2005	25	0.7793	0.0024
BZBT 9a.40	35-40	plant material	USGS-9506	>modern	-	1.5672	0.0045
BZBT 9.49	47-49	*Picea mariana* needles	USGS-9263	165	25	0.9796	0.0027
BZBT 9a.85	80-85	charcoal	Beta-417890	180	30	0.9852	0.0037
BZBT 9a.100	95-100	charred wood	USGS-9507	240	25	0.9705	0.0028
BZBT 9b.130	124-130	charred wood	USGS-9505	1885	25	0.7909	0.0023
BZBT 11.32	31-32	Unidentified plant material	USGS-9813	205	25	0.9749	0.0029
BZBT 11.56	55-56	charcoal	Beta-417888	1440	30	0.8421	0.0031
BZBT 11.116+	116- ~117	charcoal	Beta-417889	4020	30	0.6108	0.0023
BZSE 3.26	24-26	*Picea mariana* needles, *Vaccinium* spp. leaves	Beta-397860	-	-	1.1848	0.0029
BZSE 3.36	34-36	moss, leaves	LLNL-177618	>modern	-	1.7451	0.0050
BZSE 3.70	65-70	charcoal, Undifferentiated shrub leaf fragments, *Carex* spp. seed	LLNL-177619	560	25	0.9328	0.0028
BZSE 3.140+	140- ~141	charcoal	LLNL-177617	2895	25	0.6976	0.0020
BZSE 4c.44	42-44	*Sphagnum* spp. stems, *Picea needles*	Beta-415691	-	-	1.0116	0.0025
BZSE 4.56 Suppl	54-56	*V. oxycoccus* leaves, *Picea mariana* needles, undifferentiated leaf fragments, *Aulacomnium palustre* leaves & stems	Beta-399723	260	30	0.9758	0.0036
BZSE 4.69	67-69	*Picea mariana* needle, undifferentiated leaf fragment	Beta-397857	170	30	0.9868	0.0037
BZSE 4.73 Suppl	71-73	*Betula* spp. seeds, *Picea* spp. needle fragments, *Aulacomnium palustre* stems & leaves, undifferentiated shrub leaf fragments	Beta-399725	80	30	0.9979	0.0037
BZSE 4.86	84-86	charred leaf and wood fragments	Beta-397859	480	30	0.9494	0.0035
BZSE 4.93	90-93	charcoal	LLNL-177621	310	25	0.9620	0.0028
BZSE 4.130	127-130	*Picea* spp. needles, undifferentiated shrub leaves	LLNL-177620	490	35	0.9407	0.0036

SUPPLEMENTAL INFORMATION

BZSE 4.146	144-146	*Sphagnum* spp. stems, charcoal	Beta-415392	2130	30	0.7732	0.0029
BZGC 11.24	22-24	*Sphagnum* spp. stems	LLNL-176602	>modern	-	1.6362	0.0057
BZGC 11.48	48-50	*Sphagnum* spp. stems	LLNL-176603	1500	30	0.8295	0.0028
BZGC 11.55	54-55	*Sphagnum* spp. stems	LLNL-177024	1130	40	0.8689	0.0042
BZGC 11.65	64-66	*Sphagnum* spp. stems	LLNL-176604	4290	70	0.5863	0.0044
BZGC 11.76	77-78	charcoal	LLNL-177025	1870	30	0.7926	0.0028
BZGC 11.94	94-95	bulk peat	LLNL-179990	2475	30	0.7347	0.0025
BZGC 11.96	97-98	charcoal	LLNL-176605	4385	30	0.5782	0.0022

SUPPLEMENTAL INFORMATION

Figure S2. Map of landform age (cal BP) based on Bacon model output with the *wmean* values presented first and the maximum and minimum age estimates within parentheses. Green circles indicate areas that still contain permafrost. The other colors represent cores taken from different bogs. Circles without values were not age dated.

SUPPLEMENTAL INFORMATION

Figure S3. Map of permafrost thaw based on bacon model output with the *wmean* values presented first and the maximum and minimum age estimates within parentheses. Colors represent cores taken from different locations. The green circles do not have values as these sites still contain permafrost.

SUPPLEMENTAL INFORMATION

Figure S4. Carbon stocks over time by stratum with logarithmic fits. Bog parameters (polynomial fit): Intercept = -0.1551, x = 0.1196, x^2 = -0.0003. Permafrost forest parameters (logarithmic fit): a = 0.7575, b = 4.9613. Fen/marsh parameters (logarithmic fit): a = 2.266, b = 14.646.

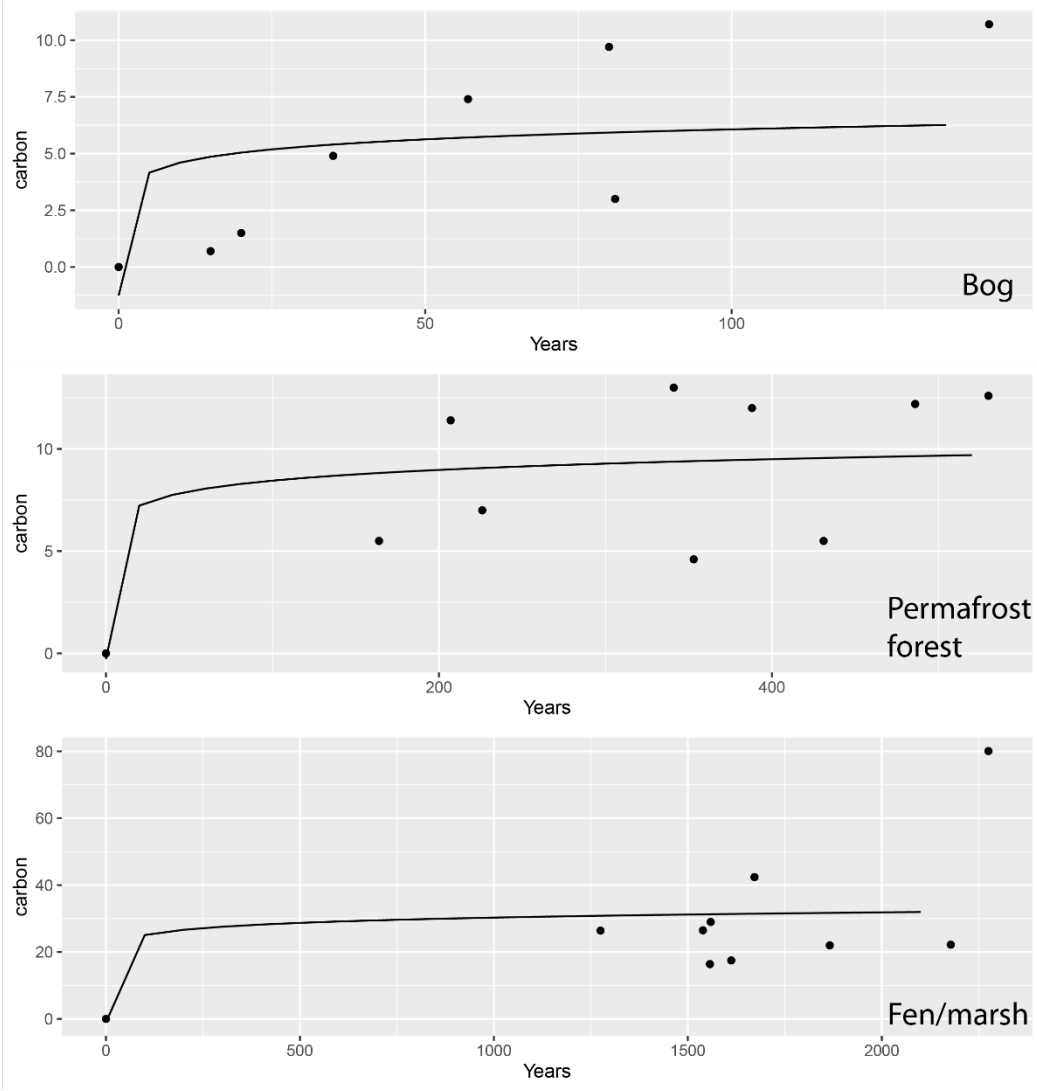

SUPPLEMENTAL INFORMATION

Figure S5. Plot of volumetric water content, which is correlated to ice content, for the mineral soil from cores taken in two places: (top) close to the young thaw feature, which had slow expansion, and (bottom) close to the intermediate thaw feature, which experienced much quicker expansion.

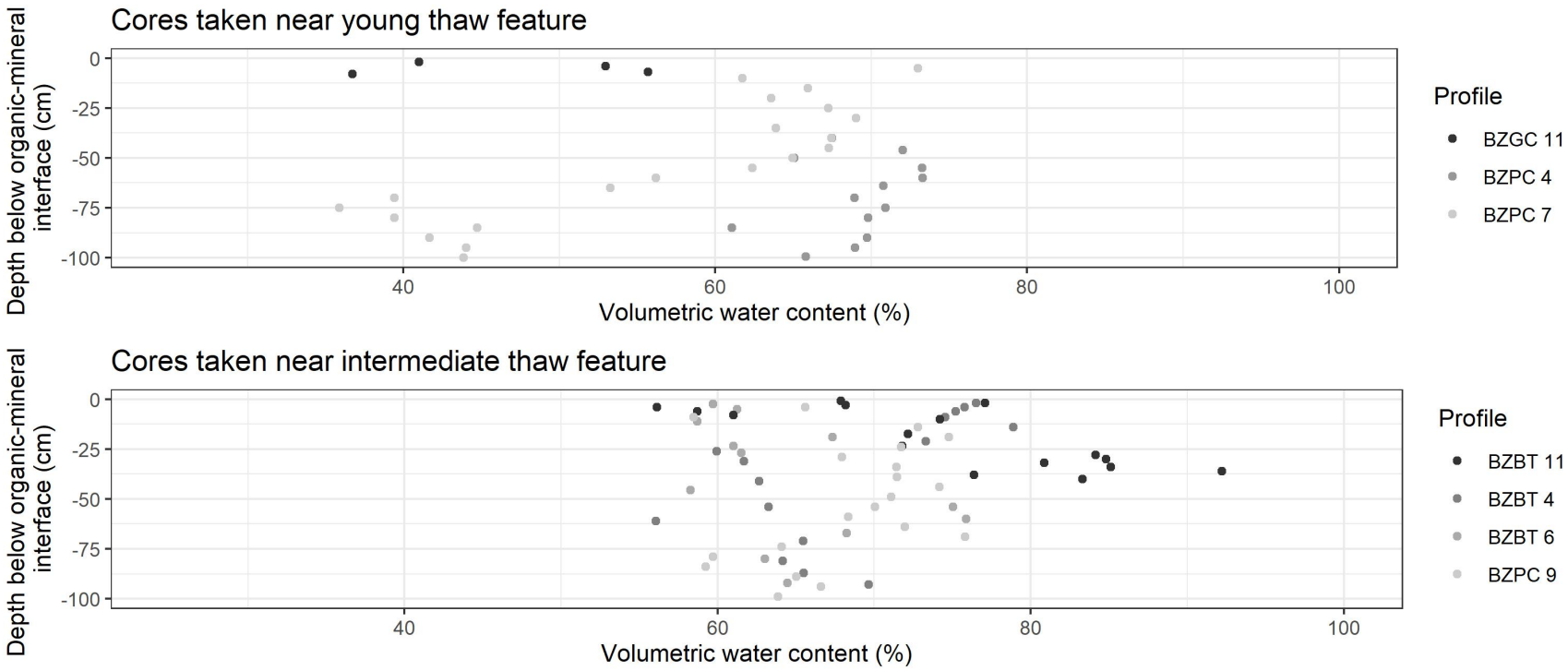

SUPPLEMENTAL INFORMATION

Figure S6. Comparison of organic soil between epigenetic permafrost (this study, APEX) and syngenetic permafrost (Innoko and Koyukuk, AK; Jones et al, 2016) for (A) C:N ratios, (B) C concentrations, and (C) N concentrations. We also found a permafrost type by horizon (Manies, 2020) interaction for Nitrogen.

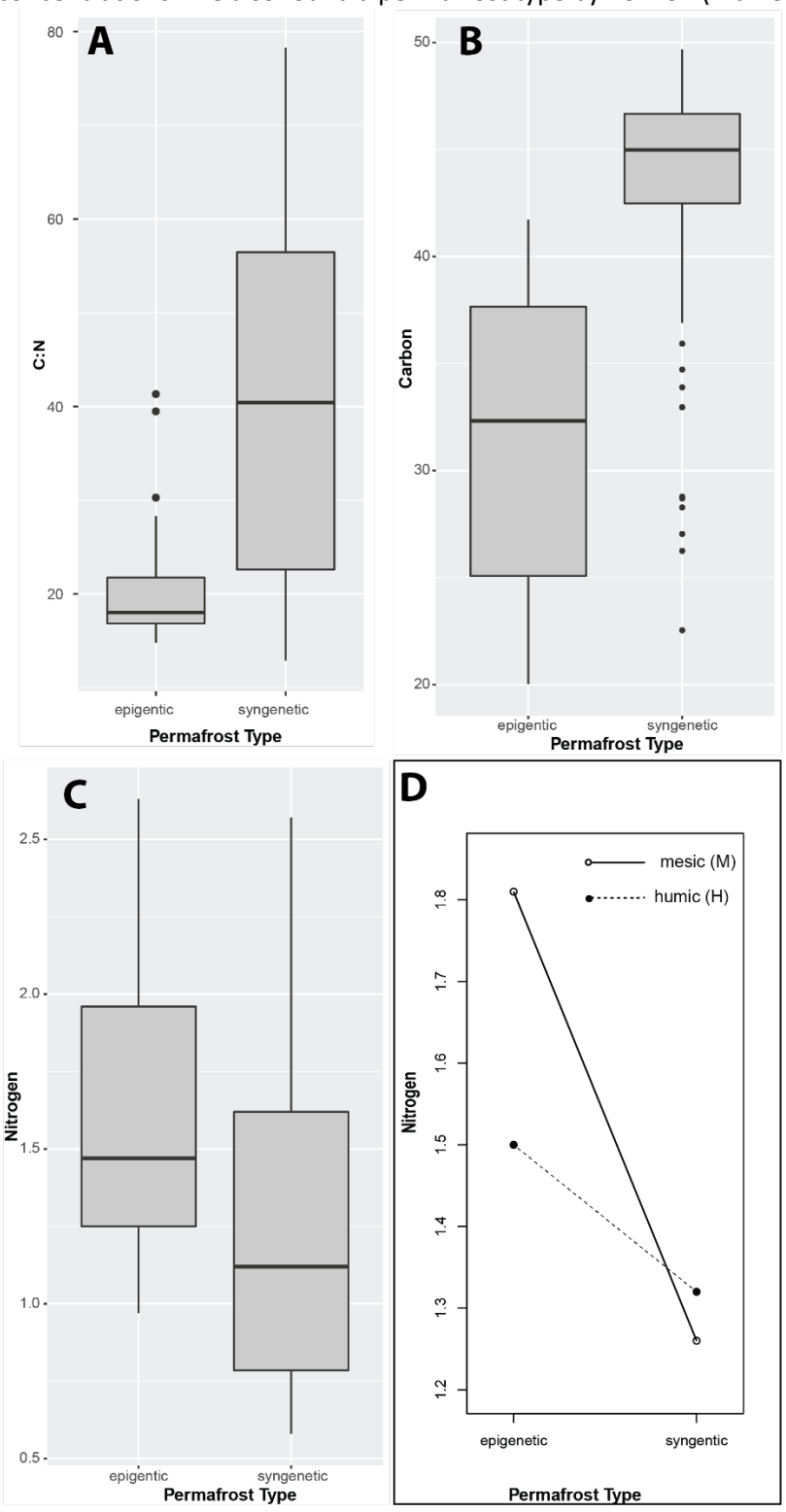

SUPPLEMENTAL INFORMATION

Figure S7. Macrofossil diagram of cores showing percentage and count data for material found within each sample.

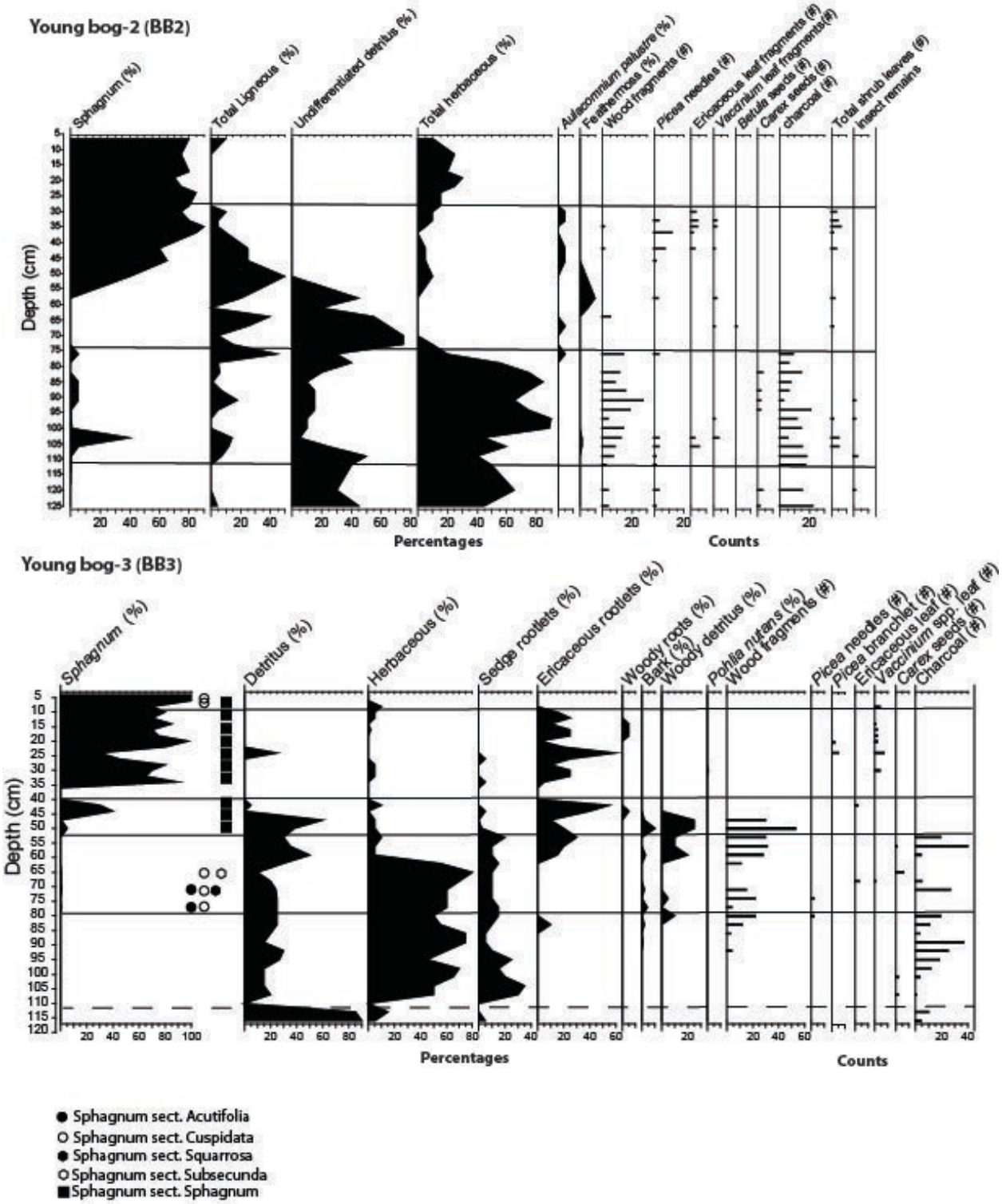

SUPPLEMENTAL INFORMATION

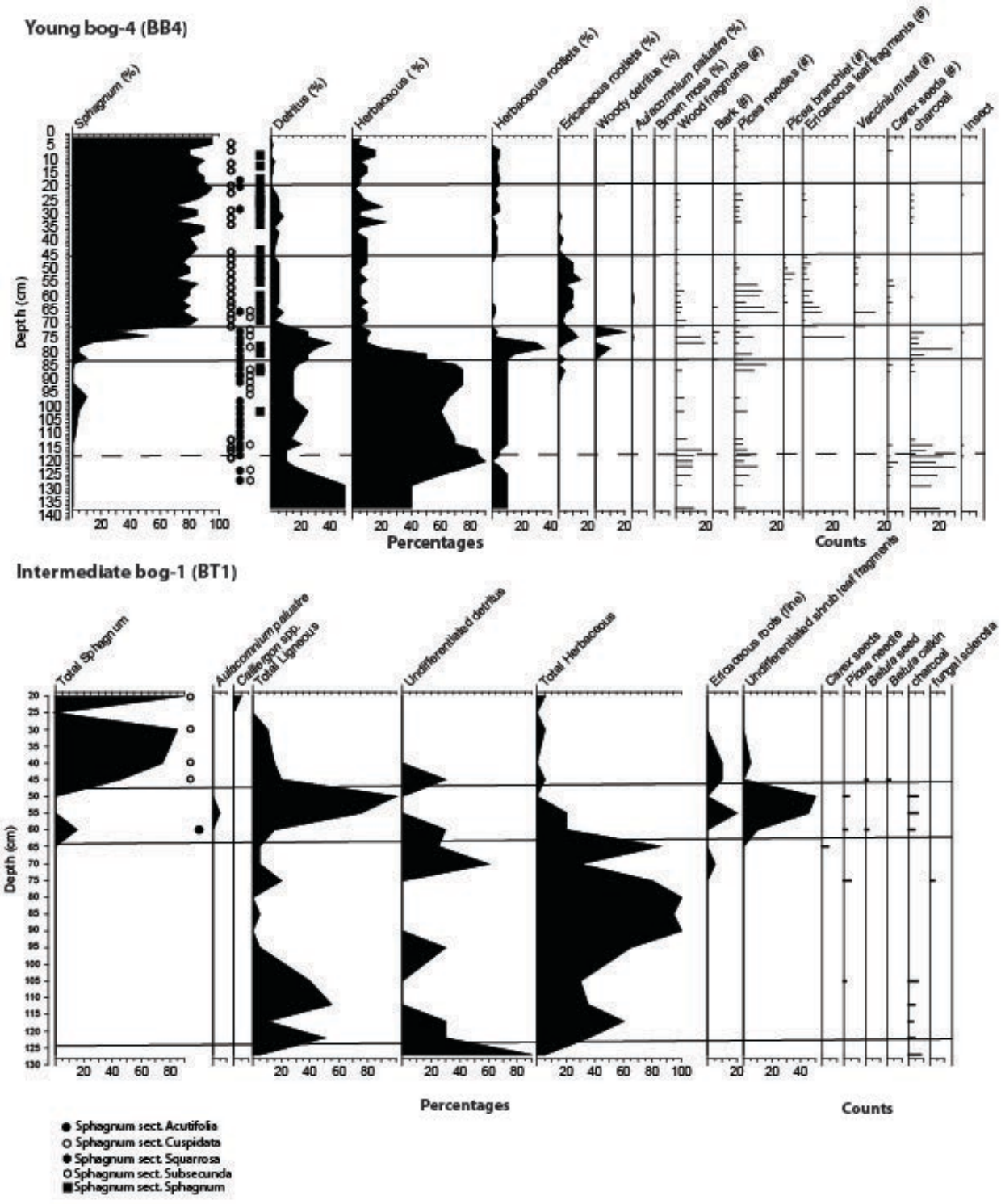

SUPPLEMENTAL INFORMATION

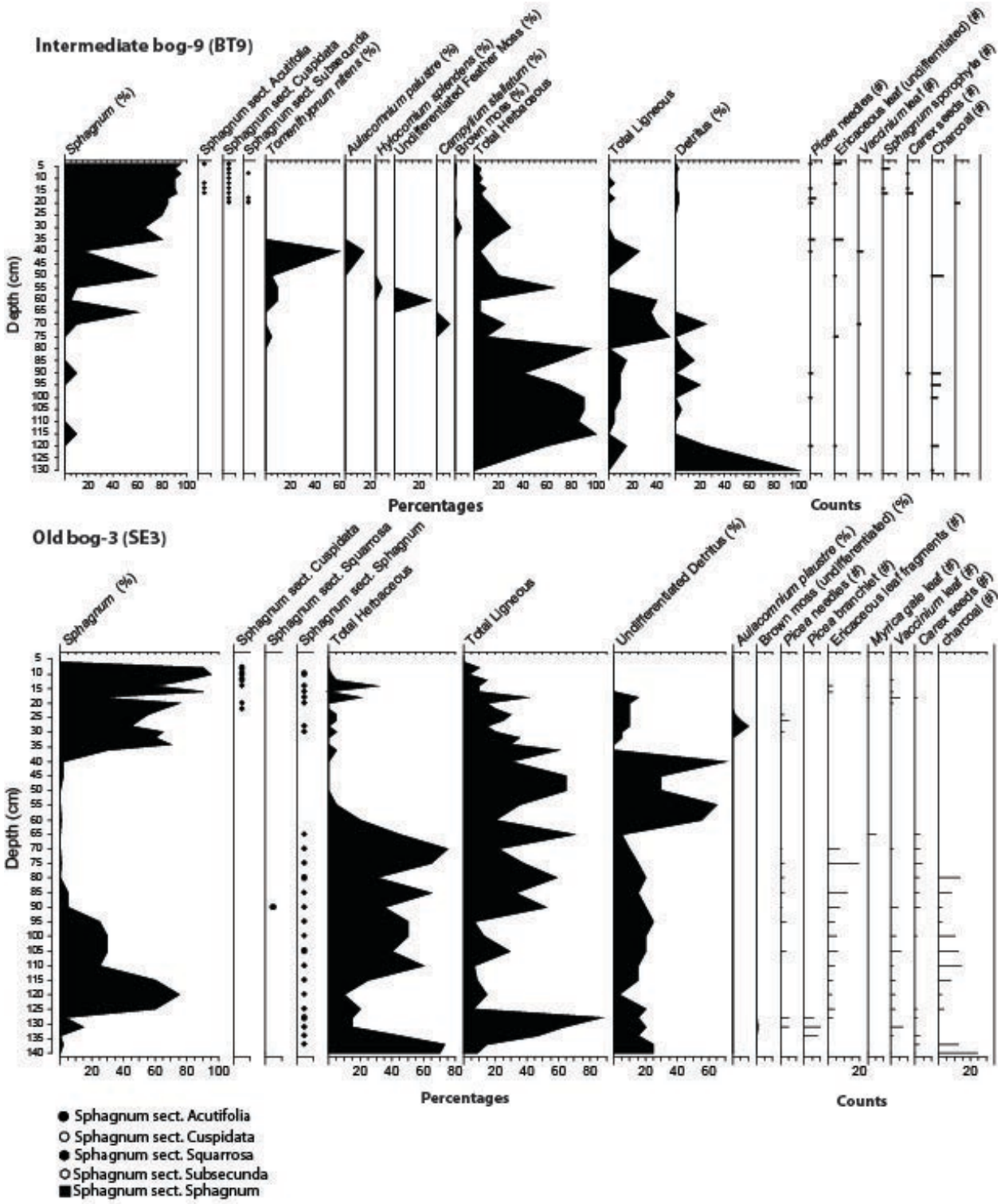

SUPPLEMENTAL INFORMATION

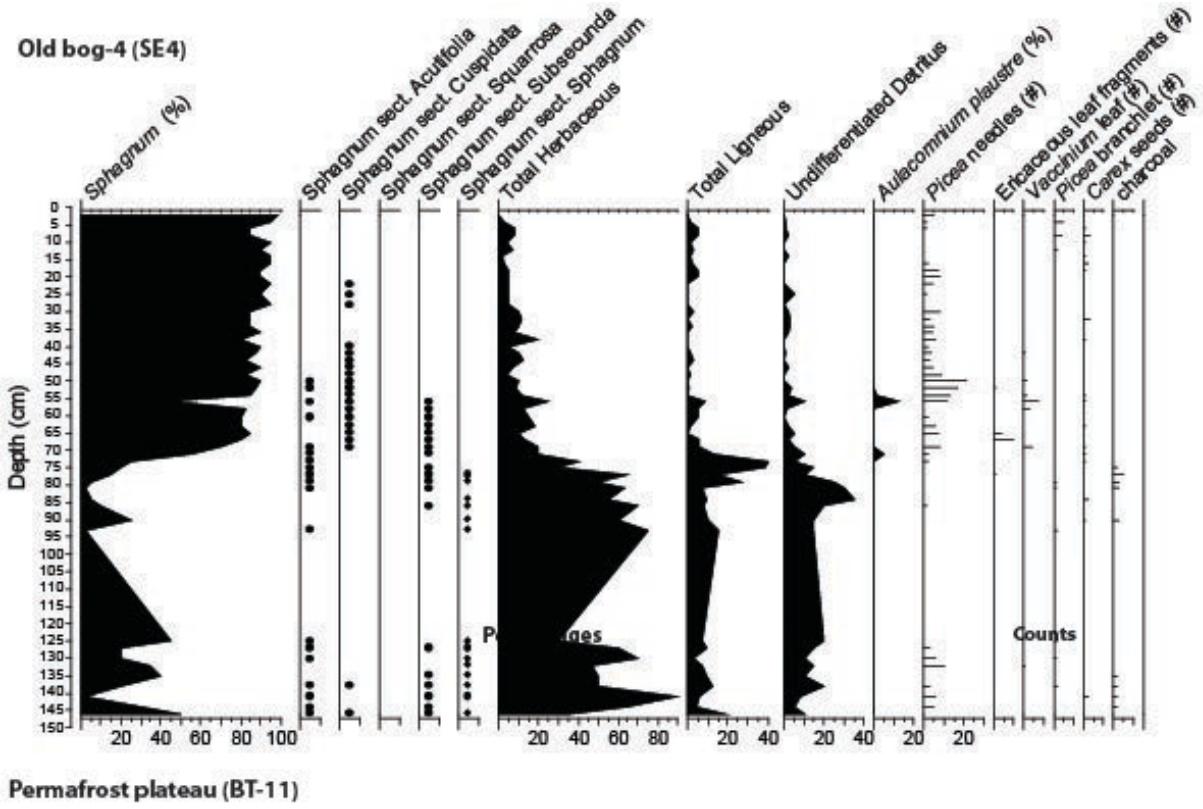

Percentages

Counts

- ● Sphagnum sect. Acutifolia
- ○ Sphagnum sect. Cuspidata
- ● Sphagnum sect. Squarrosa
- ○ Sphagnum sect. Subsecunda
- ■ Sphagnum sect. Sphagnum

SUPPLEMENTAL INFORMATION

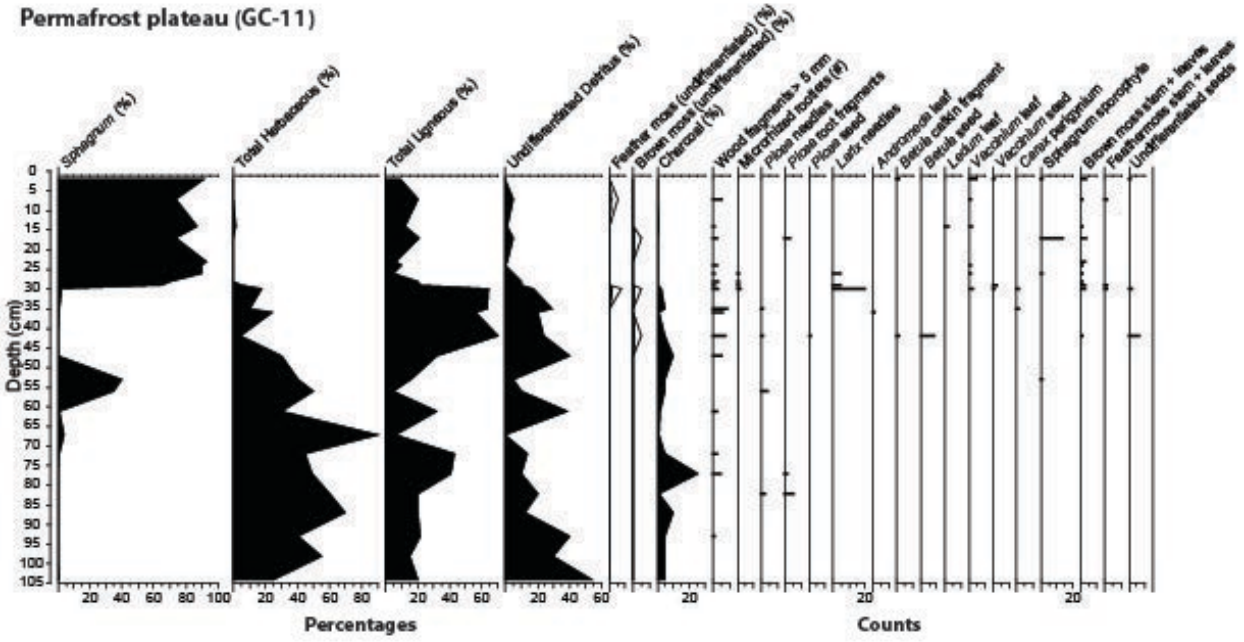

SUPPLEMENTAL INFORMATION

Figure S8. Results of Bacon age models (Blaauw & Christen, 2011) for each soil core using date of sampling for the surface and the ^{14}C dates found in Table S2.

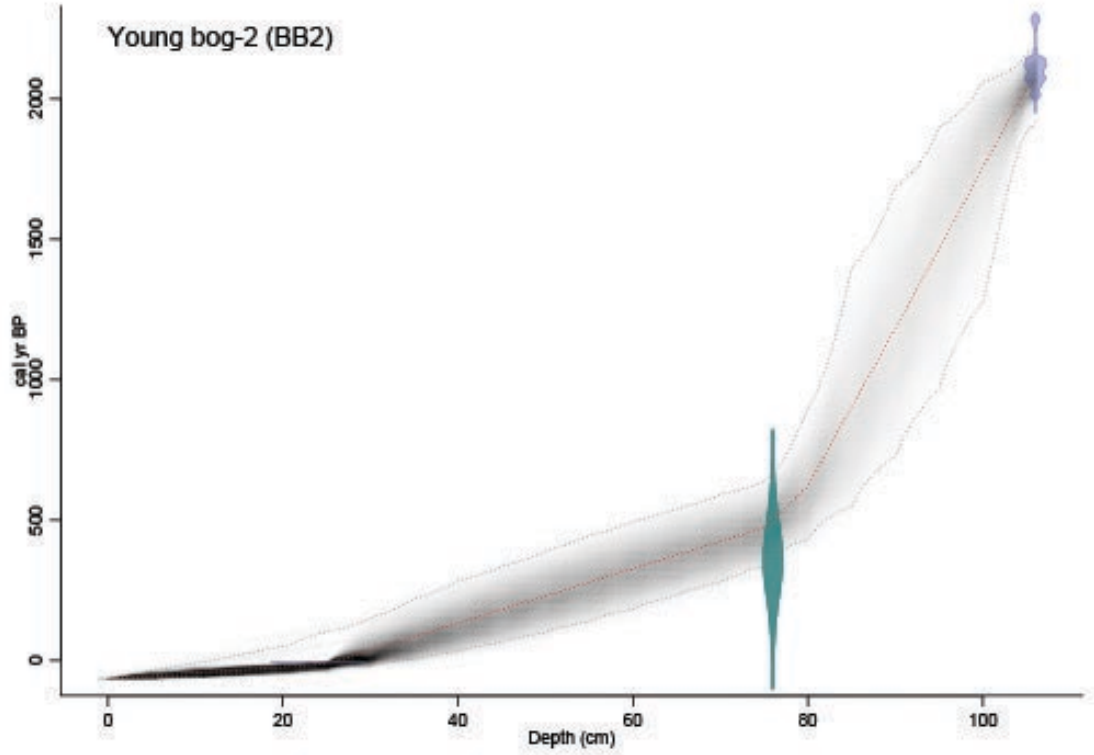

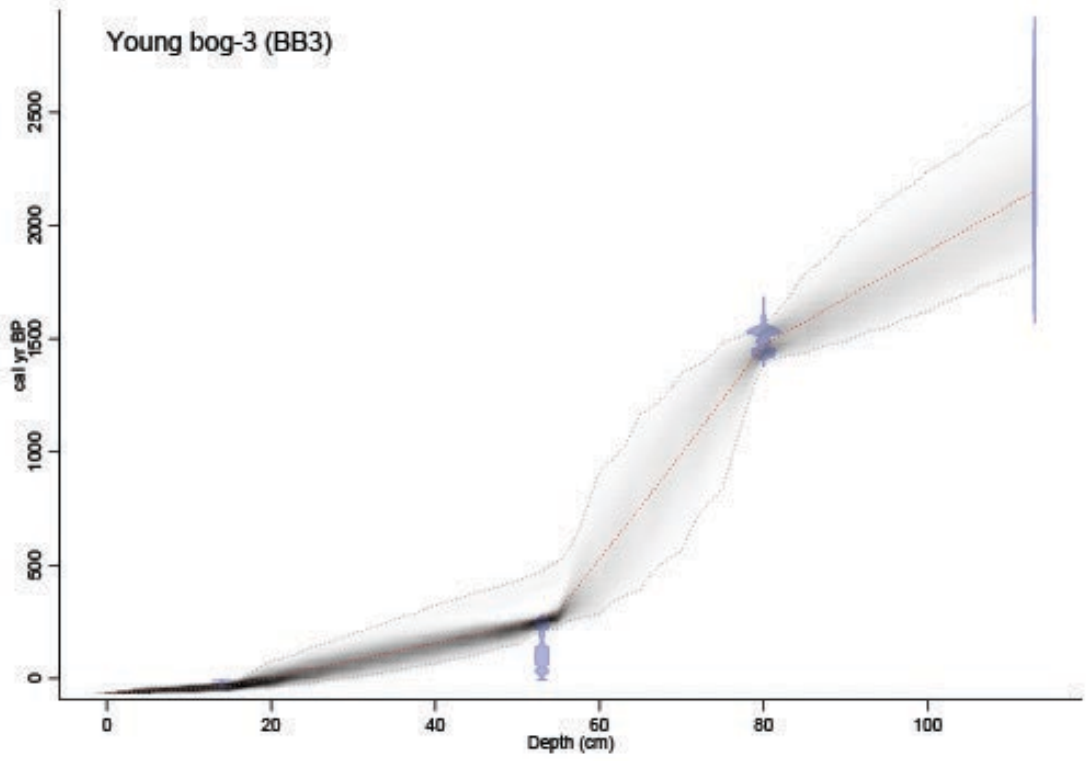

SUPPLEMENTAL INFORMATION

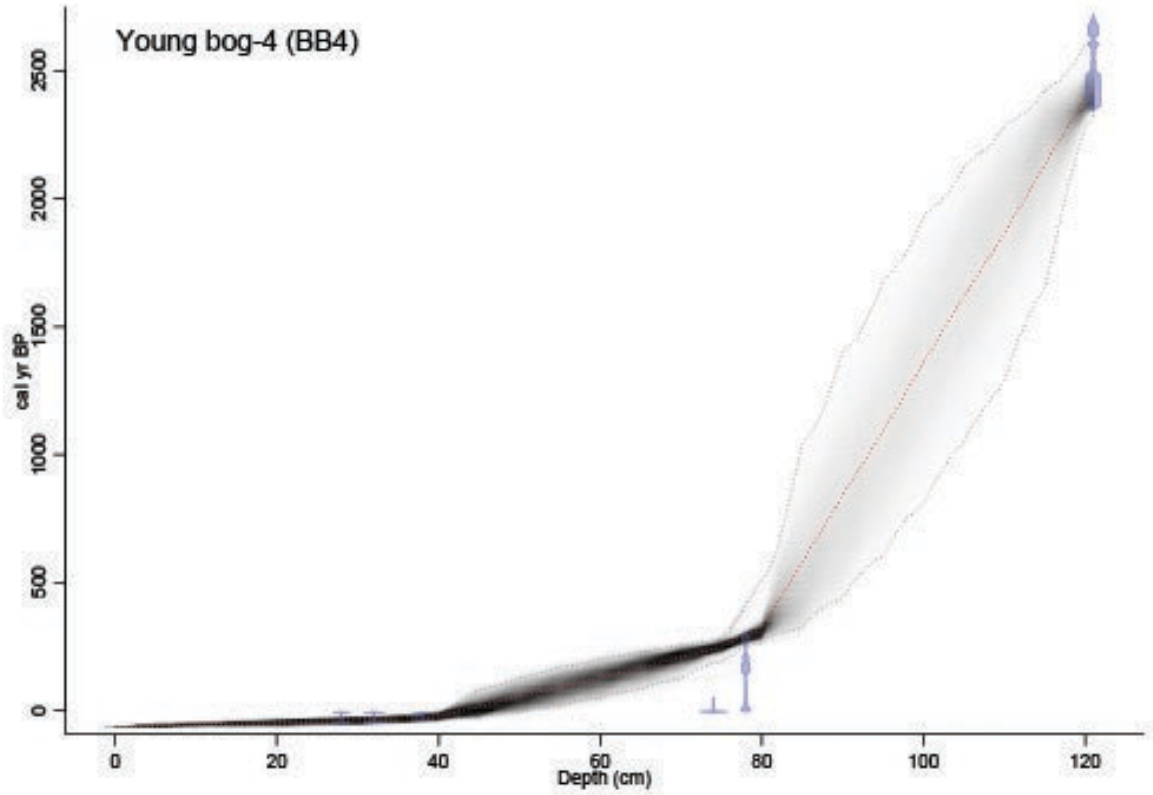

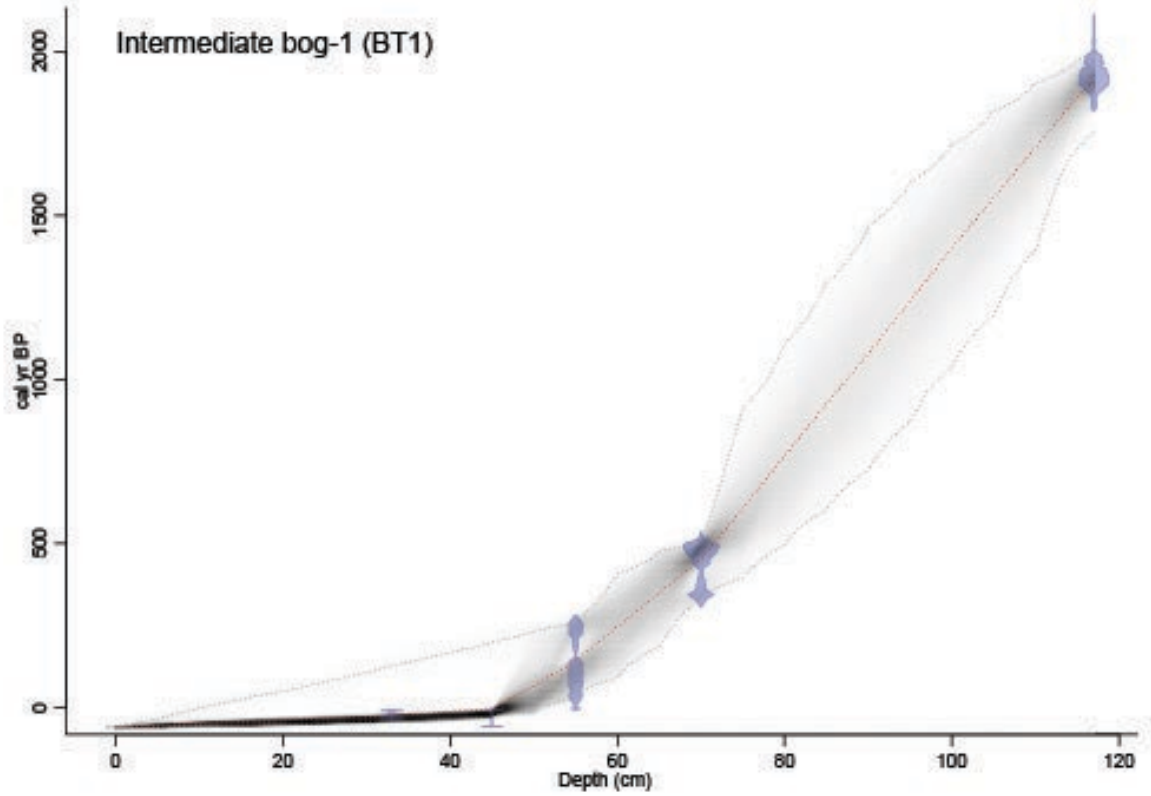

SUPPLEMENTAL INFORMATION

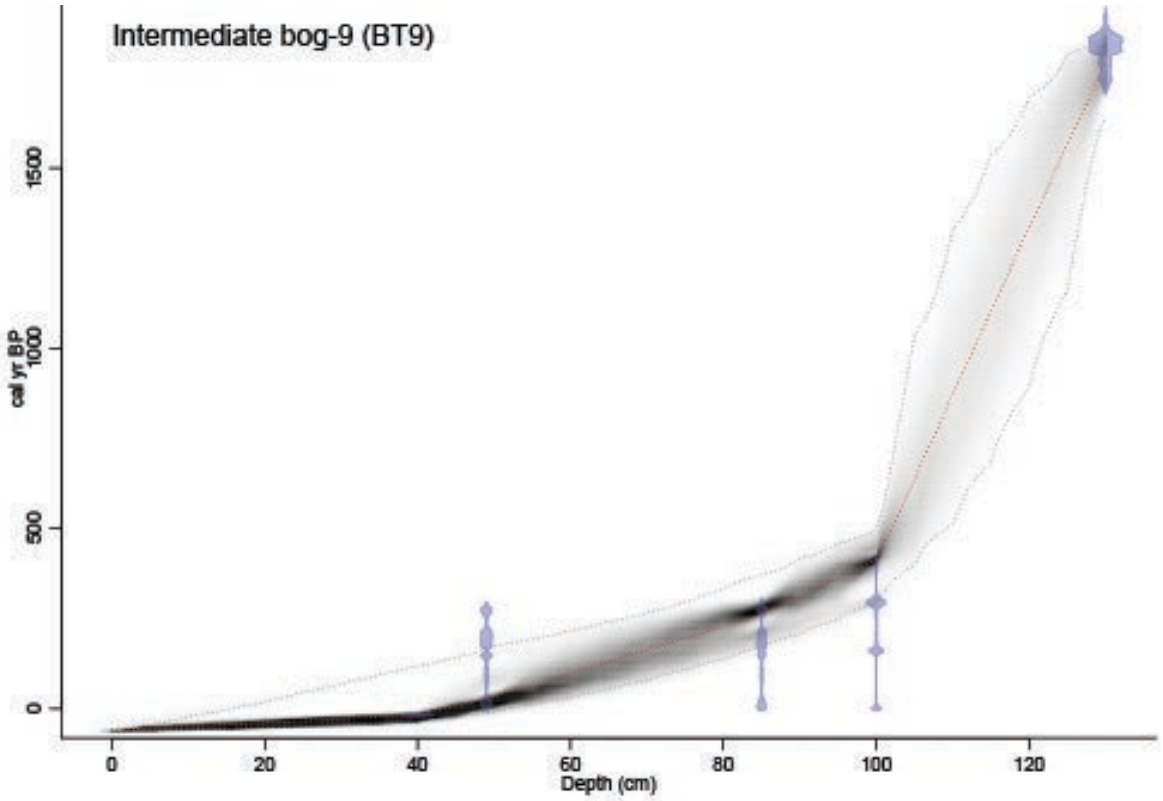

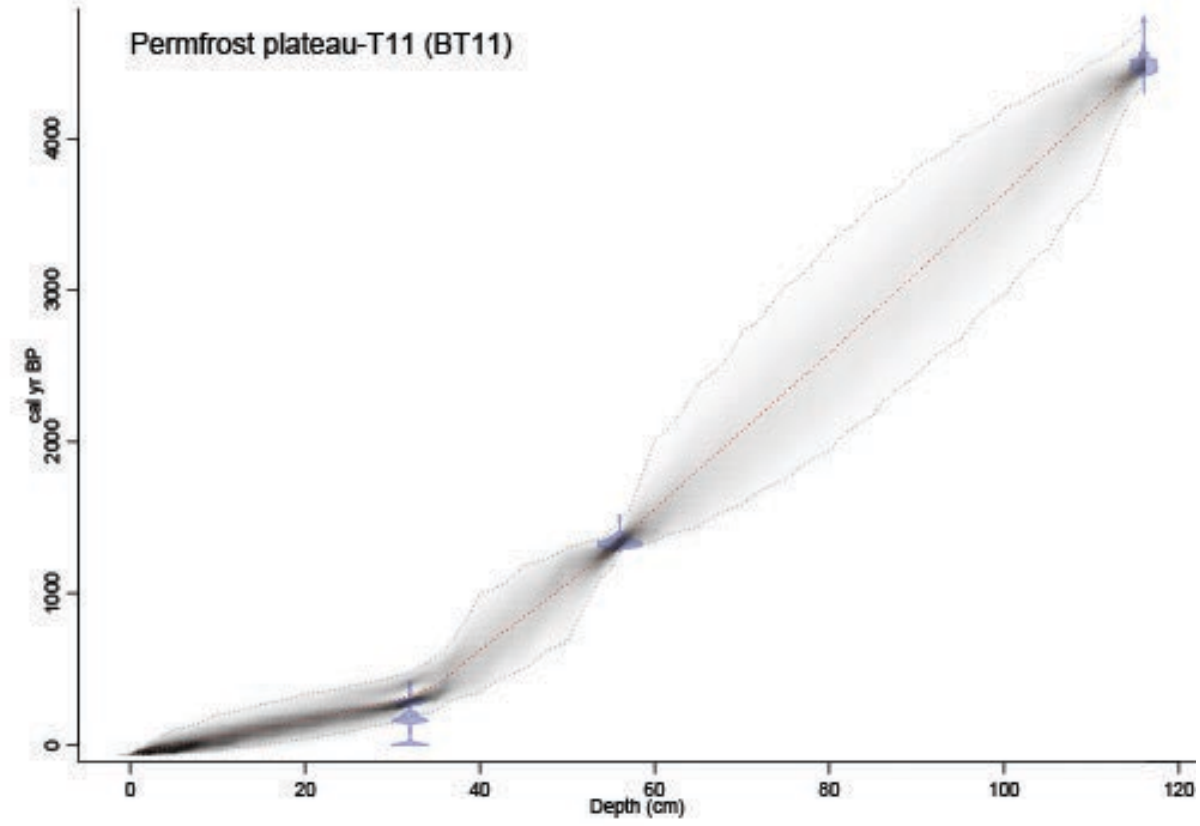

SUPPLEMENTAL INFORMATION

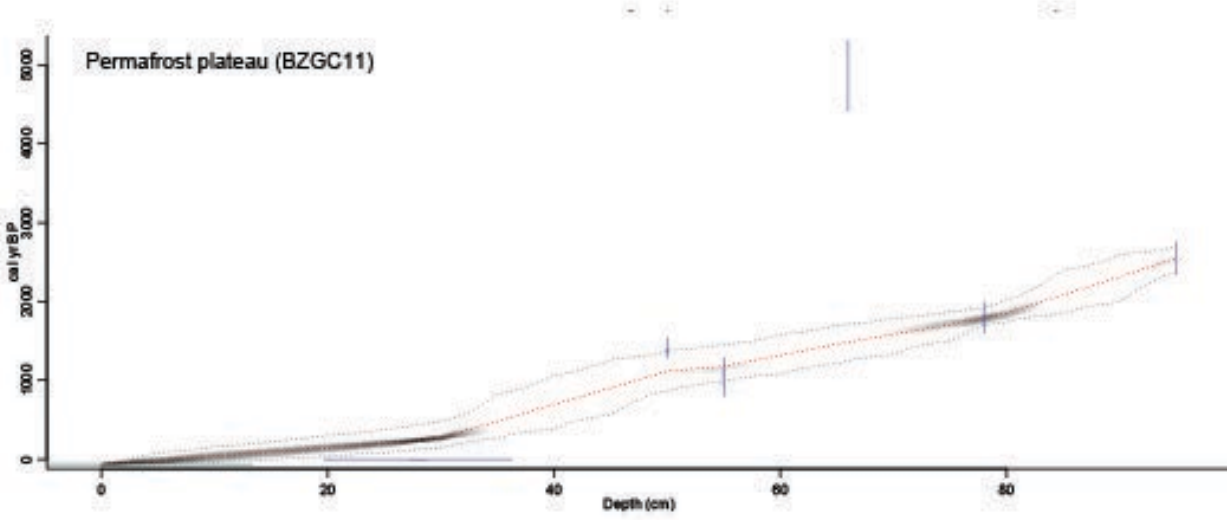

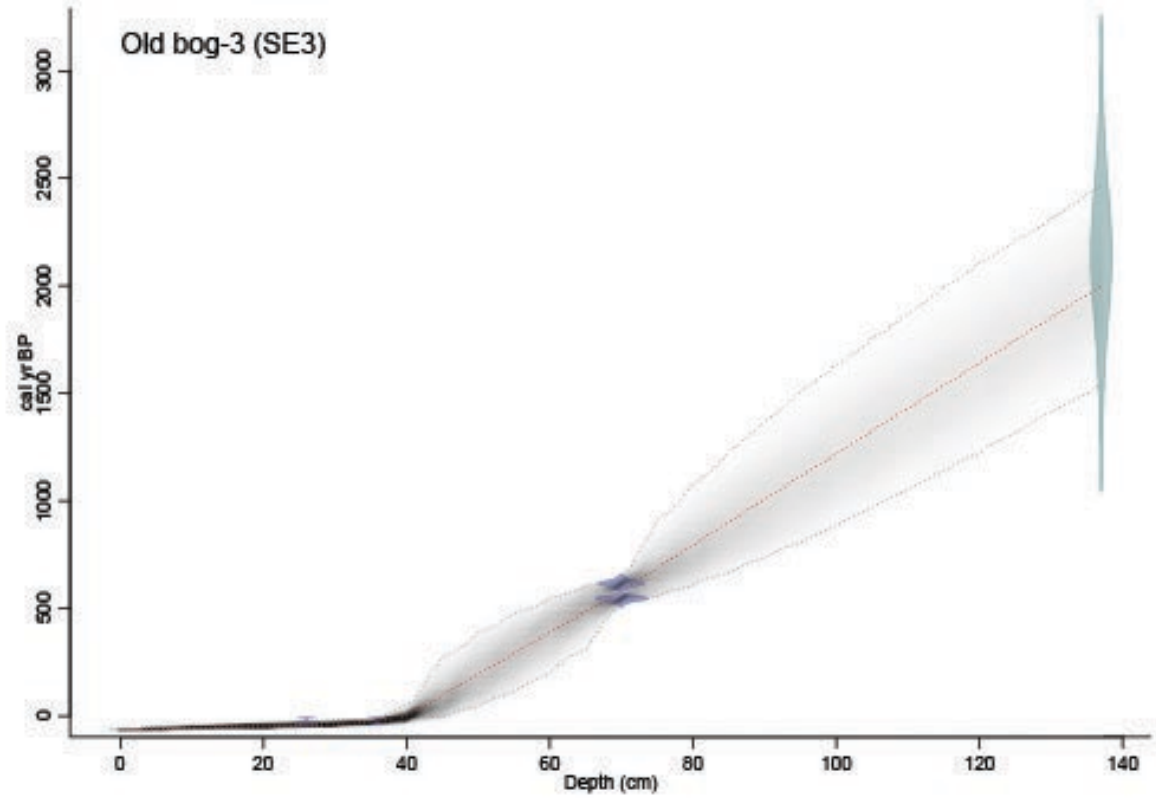

SUPPLEMENTAL INFORMATION

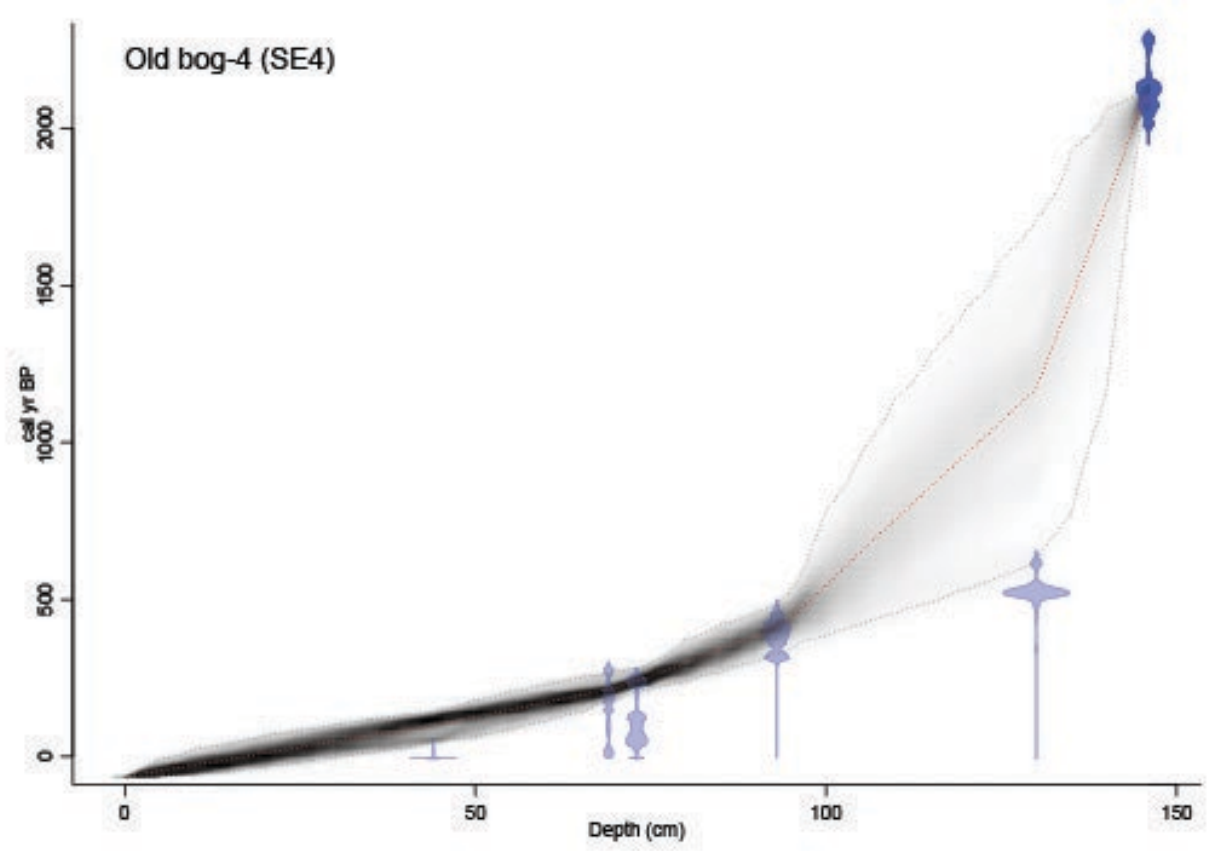

References

Blaauw, M., & Christen, J. Blaauw, M., & Christen, J. A. (2011). Flexible paleoclimate age-depth models using an autoregressive gamma process. Bayesian Anal., 6(3), 457-474

Hansson, S. V., et al. (2015). "Downwash of atmospherically deposited trace metals in peat and the influence of rainfall intensity: An experimental test." Science of The Total Environment 506–507: 95-101.

Manies, K., Fuller, C., & Jones, M. (2016). *Modeling Peat Ages Using ^{7}Be Data to Account for Downwash of ^{210}Pb*. Paper presented at the American Geophysical Union Fall Meeting, San Francisco, CA. https://ui.adsabs.harvard.edu/abs/2016AGUFM.B23C0597M.